allowed them to know the origin of their tumor. Respondents were WTP more for IHC testing when its diagnostic performance was assumed to be high. Preliminary statistical analyses examining factors linearly correlated or significantly associated with WTP did not reveal any factors clearly driving respondents' WTP.
Conclusions: In this study examining patient preferences for anatomic pathology ancillary testing, patients reported being WTP approximately $2000 for the information IHC may provide regarding tumor origin, even if this information didn't improve their long-term clincial outcome. Depending on the particular IHC work-up utilized, IHC appears to be cost beneficial in the work-up of these two groups of cancer patients.

1509 Improving Patient Safety by Examining Pathology Errors: Year 2 Findings

SS Raab, R Zarbo, S Geyer, C Jensen, DM Grzybicki. University of Pittsburgh, Pittsburgh, PA; Henry Ford Hospital, Detroit, MI; Western Pennsylvania Hospital, Pittsburgh, PA; University of Iowa, Iowa City, IA.
Background: Four institutions are currently sharing anatomic pathology error data collected for a 5-year grant sponsored by the Agency for Healthcare Research and Quality. This report details the frequency of error and the successes and failures of specific error reduction plans.
Design: Six years of cytologic-histologic correlation data have been entered into a web-based database, and these data have been used to create error reduction plans. Data collected include specimen site, type of error (sampling or interpretation), severity of error, and specific pathologist or cytotechnologist provider. Error frequencies and interobserver variability were calculated by each institution examining errors detected at other sites. Error reduction plans included the introduction of double viewing pulmonary cytology specimens, creation of specific sign-out terms for gynecologic histologic specimens, and review of thyroid aspiration specimens to determine error cause. Success of error reduction plans was monitored by determination if error reduction plans reduced errors.
Results: Frequency of error per institution for gynecologic specimens ranged from 1.7% to 9.5% of all cases correlated. Frequency of error per institution for non-gynecologic specimens ranged from 5.9% to 11.7% of all cases correlated. Pairwise institutional kappa values for agreement on error type (sampling or interpretation) ranged from 0.12 to 0.74. Some institutions thought that none of their errors resulted in patient harm whereas other institutions thought that 30% of errors resulted in patient harm. Error reduction plans had variable effect on decreasing error frequencies. Double viewing pulmonary cytology specimens had no effect on decreasing errors whereas targeting thyroid aspiration resulted in decreasing false negatives.
Conclusions: Errors occur at a high frequency and there is little institutional agreement regarding error cause and error severity. Error reduction plans have met variable success and are highly dependent on local culture. Error reduction plans designed to target specimen quality have achieved greater success than plans designed at decreasing interpretive error.

1510 Error Reduction in Specimen Labeling

RE Weisburger, CA Hodorowski, DE Zuaro, CC Black. Dartmouth Hitchcock Medical Center, Lebanon, NH.
Background: Specimen labeling errors that occur during accessioning can result in significant adverse and sentinel events. In mid-2003, our error rate had escalated to weekly occurrences. Among the most serious consequences included two separate incidents where pap smear identification was unable to be verified and 4 patients had to be called back to be re-sampled. Another incident involving a breast core biopsy was only discovered when the histologic findings did not correlate with the mammogram impression. Following these, a QA group was organized to examine the process.
Design: The major "Toyota" principles we employed were 1. No batching 2. utilize a "pull" system rather than a "push" system 3. Ensure a perfect product at hand-offs. Our specimen handling process was mapped on a blackboard beginning with the final product (a correctly labeled slide). Each step in the process was examined ending with the receipt of the specimen. Contributing factors were also examined. Redundancies (opportunities for error) in the system became apparent with this backwards or "pull" approach. All changes implemented were considered temporary until verification.
Results: It was apparent that batching at the receiving area was a probable source of error. Contributing factors included the frequency of the task, similar patient names, similar specimen types and frequent work interuptions. Labeling specimens singly at the time of accession greatly reduced the chance of adhering the wrong label. Confusion between similar specimens and names was eliminated by working with just one specimen until completion. Accessioners were sharing a label printer which required walking to the shared printer to retrieve ones own labels. In addition to the elimination of batching, we invested in separate label printers for all accessioners.
Conclusions: Initially there was some staff resistance to the new no batching policy due to perceptions that batching was more efficient. However, after a 12 month period, labeling errors have dropped from 1-2 per week to 2 in 12 months. Both of these errors were caused by new trainees batching their work. We plan to apply the principle of no batching to other areas within anatomic pathology in the future.

Techniques

1511 Mutational Analysis of *CEBPA* in Acute Myeloid Leukemia: An Integrated Approach Using Denaturing and Non-Denaturing Capillary Electrophoresis and Direct Sequencing

B Barkoh, D Jones, M Jaju, K Vadlamudi, E Lopez-Alvarez, E Estey, H Kantarjian, R Luthra. M.D. Anderson Cancer Center, Houston, TX.
Background: C/EBP$^{\alpha}$ (CCAAT/enhancer binding protein-alpha) is a transcription factor that regulates myeloid differentiation. Mutations in *CEBPA* are present in approximately 10-15% of intermediate risk AML and were shown to be a favorable prognostic factor. The variety of mutations that occur in *CEBPA* make rapid definitive assessment of mutational status difficult.
Design: We developed a mutational analysis method for *CEBPA* using capillary electrophoresis (CE) under denaturing (GeneScan sizing) and non-denaturing (single strand conformational polymorphism-SSCP) conditions. Genomic DNA was extracted from the bone marrow or blood of 40 patients with AML (FAB: 3-M0; 10-M1; 16-M2; 9-M4; 1-M7; 1-MDS). The N-terminal (550 bases) and C-terminal (680 bases) regions of *CEBPA* were amplified in separate PCR reactions, using FAM-labeled forward primers and HEX-labeled reverse primers. PCR fragments were analyzed by CE and confirmation of the detected mutations was done by direct sequencing.
Results: SSCP/CE analysis detected eight (20%) N-terminal fragments and ten (25%) C-terminal fragments with mobility shifts as compared to wild-type. Sequencing analysis revealed six (15%) samples with N-terminal mutations (four single base insertions and two single base deletions) and ten (25%) samples with C-terminal sequence changes (five polymorphisms and five changes, involving deletions, insertions and duplications of various number of bases). Comparison of SSCP with sequence analysis revealed that 16 of 18 samples with mobility shifts had sequence variations. Careful review of the two discrepant cases by direct sequencing revealed sequence variations in only one strand. The remaining samples without mobility shifts in SSCP/CE analysis were also unmutated by sequence analysis. Fragment sizing by Genescan was useful in determining the number of bases involved in sequence variations larger than two bases.
Conclusions: These results indicate that the use SSCP/CE in tandem with GeneScan fragment size analysis are reliable and rapid initial screening methods for mutation detection in *CEBPA*. Despite the wide spectrum of mutations that occur in *CEBPA* in AML patients, there was a high concordance rate between direct sequencing and SSCP. Therefore, this approach will reduce the time and money spent on mutation detection using direct sequencing by at least 70%.

1512 High Sensitivity and Specificity of FISH in Routine Detection of t(14;18)(q32;q21) and t(11;14)(q13;q32) in Formalin-Fixed Paraffin-Embedded (FFPE) Tissue Sections Using Automated Morphometric Image Analysis

TS Barry, HC Hwang, LC Goldstein, H Yaziji, AW Hing, AM Gown. PhenoPath Laboratories and IMPRIS, Seattle, WA.
Background: PCR detection of the t(14;18)(q32;q21) and t(11;14)(q13;q32) has remained the primary method for confirming the presence of chromosomal translocations characteristic of follicular (FL) and mantle cell lymphomas (MCL), respectively. However, the sensitivity of these PCR-based assays is suboptimal in FFPE tissues with reported rates of ~60-75% for t(14;18) and ~30-40% for t(11;14). We assessed the sensitivity and specificity of 2-color interphase FISH for the detection of t(14;18) and t(11;14) in archival FFPE tissue sections using morphometric image analysis.
Design: All lymphoid tissues were examined morphologically and fully characterized by immunohistochemistry. All MCLs showed nuclear cyclinD1 protein expression. Deparaffinized tissue sections were incubated with Vysis probes (IgH gene;14q32;Spectrum Green and either bcl-2 gene;18q21;Spectrum Orange or cyclinD1 gene;11q13;Spectrum Orange) following digestion/pretreatment. Morphometric analysis was performed using a MetaSystems™ imaging system with extended focus/tile sampling methodology. Signals in close proximity (<2 pixels) were considered positive and the percentage of positive tiles was calculated for each case. Case positivity was defined as 3 standard deviations above the mean of a translocation-negative group.
Results: In t(14;18)(q32;q21) FISH assays, 31 of 34 FLs showed a t(14;18), whereas none of the reactive lymph nodes (n=7) or non-follicular, B-cell lymphomas (n=23; including 2 CLL/SLLs, 6 MZBCLs, 11 MCLs) contained a t(14;18). The sensitivity and specificity of the t(14;18) FISH assay was 91.2% and 100%, respectively. A t(14;18) could be demonstrated in 2 FLs undergoing histologic transformation to large B-cell lymphoma and in a single FL showing marginal zone differentiation. 1 of 7 de novo DLBCLs showed a t(14;18) by FISH. In t(11;14)(q13;q32) FISH assays, 21 of 21 MCLs contained a t(11;14), whereas none of the reactive lymph nodes (n=10) or non-mantle cell, B-cell lymphomas (n=16; 2 CLL/SLLs, 3 DLBCLs, 11 FLs) contained a t(11;14). Both the sensitivity and specificity of the t(11;14) FISH assay were 100%.
Conclusions: 2-color interphase FISH is a rapid, highly sensitive and specific method for the routine detection of t(14;18) and t(11;14) in archival FFPE tissues using automated morphometric analysis and offers a significantly higher rate of detection than that reported for standard PCR.

1513 High Sensitivity and Specificity of FISH in Routine Detection of t(X;18)(p11.2;q11.2) in Synovial Sarcomas (SS) Using Formalin-Fixed Paraffin-Embedded (FFPE) Tissue Sections and Automated Morphometric Image Analysis

TS Barry, J Terry, TO Nielsen, HC Hwang, LC Goldstein, AM Gown. PhenoPath Laboratories and IMPRIS, Seattle, WA; British Columbia Cancer Agency, Vancouver, BC, Canada.

Background: Synovial sarcoma (SS) is a diagnostically challenging, malignant mesenchymal neoplasm which accounts for roughly 5% of soft tissue tumors. Although immunohistochemistry plays a crucial role in the diagnosis of synovial sarcoma, markers used to define this sarcoma are not entirely specific. RT-PCR has been the method of choice for detection of t(X;18). We assessed the sensitivity and specificity of two-color interphase FISH for the detection of t(X;18) in FFPE tissue sections using morphometric image analysis.

Design: All sarcomas (n=78) were evaluated morphologically and immunohistochemically. 24 of the 42 SS cases had been confirmed to contain a t(X;18) by cytogenetic or RT-PCR analysis. 66 of the 78 tumors were contained within a single tissue microarray, constructed from archival FFPE tissue samples that were referred to the British Columbia Cancer Agency. Deparaffinized tissue sections were incubated with Vysis SYT Translocation breakapart probe pair following digestion/pretreatment. Automated quantitative morphometric analysis was performed using the MetaSystems™ imaging system with extended focus/tile sampling methodology. Signals within tiles were stratified according to proximity, and those tiles containing signals which were separated by 10 or more image pixels were considered positive. The percentage of positive tiles was then calculated. The threshold for positivity was established from a group of non-synovial sarcoma cases which did not contain the translocation of interest. A positive case was defined as one in which the percent of positive tiles detected was > 3 standard deviations above the mean of this negative control group.

Results: In the FISH assays, 35 of 42 SS cases showed a t(X;18)(p11.2;q11.2), whereas none of the 36 non-synovial sarcoma cases contained a t(X;18)(p11.2;q11.2). The sensitivity and specificity of the t(X;18) FISH assay were 83.3% and 100%, respectively.

Conclusions: Two-color interphase FISH is a rapid, highly sensitive and specific method for the routine detection of t(X;18)(p11.2;q11.2) in archival FFPE tissues using an automated morphometric analysis and provides a rate of detection similar to that reported in conventional RT-PCR assays.

1514 Identification of the Relative Levels of Gene Expression of Androgen Receptor (AR) in 60 Different Tumor Types

D Baunoch, MW Moore, ME Reyes, BW Tirtorahardjo, ML Opel, A Au, G Krause, A Tassin, NB Edejer, J Haut, X Ma, M Erlander. US Labs, Irvine, CA; Arcturus, Mountain View, CA.

Background: Gene expression profiling is a powerful new technology capable of measuring the relative levels of transcription for genome wide gene expression. We have evaluated the relative levels of expression of Androgen Receptor (AR) gene across 550 tumors, representing over 60 tumor types. AR is believed to function as a transcriptional regulator in the synthesis of male hormones. AR is a common target for immunohistochemistry and its immunohistochemical expression is documented in prostate, skin, oral mucosa, osteosarcoma, and prostatic adenocarcinomas.

Design: For each case, a single 5um section was stained, visualized, and pure tumor populations were obtained by either manual dissection, or laser capture microdissection (Arcturus). Total RNA was extracted using a silica spin column-based extraction method (Arcturus) and was assessed using quantitative PCR (Taqman, ABI), with primers specific for B-actin transcription. Only samples with greater than 10ng of RNA were amplified using a modified RNA polymerase 2-round amplification protocol (Arcturus). Amplified RNA was labeled with Cy5, through conjugation with an Aminoallyl dUTP incorporated during amplification. A total of 5 ug (10ug for FFPE samples) of amplified, labeled RNA was hybridized to a custom 22,000 gene microarray (Agilent). This array was designed to accommodate both Fresh and FFPE samples, and contains a probe set biased for the 3region of the RNA transcript.

Results: Presented are the relative expression levels of AR mRNA across over 60 tumor cancer types. Consistent with results previously reported, we have observed high levels of AR mRNA in adenocarcinomas of the prostate. Additionally, we have also observed levels comparable to those seen in prostatic adenocarcinomas in a subset of hepatocellular carcinoma and adenocarcinomas of the the endometrium.

Conclusions: While the expression of specific proteins is often used to identify the site of tumor origin, the distribution and range of protein expression is often poorly understood. These studies attempt to examine the range and distribution of gene expression across a broad range of tumors, in the case of AR expression, we have found a consistent level of AR mRNA expression in a subset of hepatocellular carcinoma and adenocarcinomas of the the endometrium. These expression patterns may be useful in cases where the differential diagnosis includes these tumor types.

1515 Fast Computerized Texture Analysis in Pancreas Cytology without Accurate Nuclear Segmentation

M Bitar, H-S Wu, A Szporn, D Burstein, J Gil. Mount Sinai School of Medicine, New York, NY.

Background: Computerized image analysis of chromatin texture would be a fast and inexpensive ancillary method in the diagnosis of malignant cells. The main obstacle is that the nuclear segmentation required by most texture analysis procedures cannot be dependably achieved by automatic means. We have developed a method that requires only simple threshold segmentation against the approximate outline of nuclear clumps.

Design: FNA pancreatic cytology smears exhibiting benign and carcinomatous cells were chosen. Computerized image analysis was done by newly developed programs. Areas showing only benign or malignant cells were stored. By an interactive thresholding procedure approximate areas occupied by nuclei were delimited without efforts to outline single cells reasoning that the dark chromatin clumps would have recognizable properties in the frequency domain. The excluded background areas of the original image were filled with the intensity of threshold and the Hamming window was used to avoid Gibbs phenomenon before taking the 2-D Fourier transform. By circularly averaging the 2-D spectral, a modified 1-D power function is obtained. The diagnostic parameter is defined as the ratio of the total powers in two predefined low frequency bands with one included in the other. The ratio is significant in simulated model discriminating between nuclei with different size of clumps [1].

Results: The power ratios revealed large variability among benign cells but great similarity for malignant clusters of cells analyzed (Fig 1), which mostly were outside the range of benign cells.

Conclusions: Our observations indicate that the texture of nuclear chromatin in Pap-stained cytology smears has properties identifiable by computerized image analysis that can be extracted without need to perform an accurate segmentation. This approach could be automated, can be performed on routine slides and would be helpful in adding an objective component to difficult diagnoses, in a way similar to the widely used immunostains.

Ref:

[1]. H.-S. Wu, J. Gil, L. Deligdisch and T. Kalir, " Characterization of ovarian nuclei with the parameter of power ratio," Microscopy Research and Technology, 2004, in press.

Figure 1. Power ratios of 2 benign and 2 malignant cases

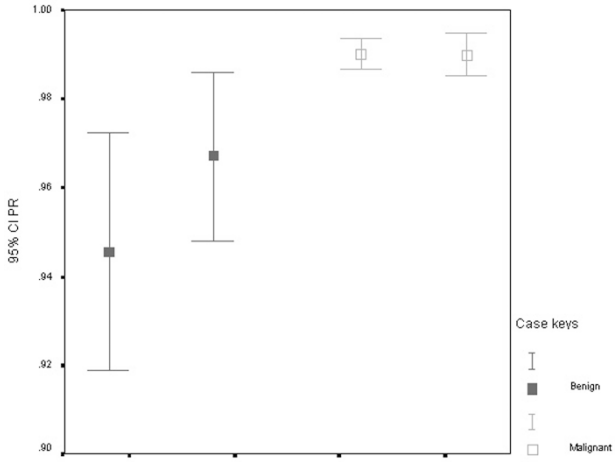

1516 The Use of a Cytokeratin 7/CDX-2 Cocktail in the Work-Up of Adenocarcinoma of Unknown Origin

KJ Bloom, D Helling, A Kyshtoobayeva, R Satyadev. ChromaVision Medical Systems, Irvine, CA; US Labs, Irvine, CA.

Background: The use of multicolor immunostain cocktails has been primarily confined to the research setting with limited routine clinical use. Double and triple immunostains are practical for pathologists and histotechnologists, reducing errors, reagent costs, time and tissue requirements. Designing clinical cocktails is non-trivial and requires the ability to match antibodies with similar pre-analytical requirements. Many algorithms have been proposed for the work-up of adenocarcinomas of unknown origin and most include assessing the expression of cytokeratins 7 and 20. We describe a double immunostain consisting of CDX2 and cytokeratin 7. CDX2 is a homeobox gene, which shows strong nuclear expression throughout the small and large intestine. More variable expression has been described in a variety of primary sites, usually with tumors showing mucinous differentiation. We describe our experience with this cocktail.

Design: Sixty eight consecutive consultations sent to US Labs for the evaluation of adenocarcinoma of unknown origin were immunostained for a variety of immunohistochemical markers including a CDX-2/CK 7 cocktail (Biocare, Walnut Creek, Ca) and CK 20 (DakoCytomation, Carpinteria, Ca). The CDX-2 was visualized with DAB (DakoCytomation) and the CK 7 was visualized with Vulcan red (Biocare).

Results: 68 tumors showed nuclear expression of CDX-2. Thirteen tumors showed expression of CK20 but no expression of CK7, (11 colon and 2 gastric carcinomas). Twelve tumors showed no expression of CK7 or CK20 (3 neuroendocrine, 2 gastric, 1 cholangio, 1 pancreatic, 1 colonic and 1 squamous carcinoma, and 3 NOS). Twenty-seven tumors showed co-expression of CK7 and CK20 (12 gastric, 12 pancreatic, 1 small bowel and 2 NOS). Sixteen tumors showed expression of CK7 but not CK 20 (6 pancreas, 2 gastric, 2 lung, 1 esophageal, 1 ovary, 1 endometrial and 3 NOS).

Conclusions: CDX-2 is an important new immunohistochemical marker. It can be effectively and practically combined with CK7 as a double immunostain in the work-up of adenocarcinoma of unknown origin. This double stain is cost effective, time efficient and tissue sparing.

1517 Strategy for Resolution of Pathology Specimen Quality Control Issues, Including a Novel mtDNA Hybridization Test

ZM Budimlija, DA Popiolek, P Illei, BA West, M Prinz. the NYC Office of Chief Medical Examiner, New York, NY; New York University School of Medicine, New York, NY.

Background: Tissue contamination detected in paraffin blocks or histological sections, and laboratory specimen mix-up are well recognized problems in surgical pathology. These issues arise even though extreme care is taken to avoid them. If a potential quality problem is suspected, it presents a challenge to the pathologist and, if not resolved may result in inappropriate therapy, or at least in additional diagnostic procedures. Thus accurate identification of the source of the tissue in these circumstances is crucial. This study assesses the effectiveness of two methods used in forensic investigation for identity testing in a clinical laboratory.

Design: Twelve cases, in which the source of tissue was uncertain, were submitted to the Forensic Biology of the NYC Office of Chief Medical Examiner for genetic identity testing. The clinical scenarios were: possible tissue contamination (6 cases), identity of biopsy tissue questioned by patients (3 cases), suspicion of malignant tissue having been introduced by a transplanted organ (2 cases), laboratory biopsies mix-up (1 case). The isolation of the tissue in question (paraffin embedded or frozen tissue) was performed by needle/scalpel scraping, and/or laser-capture microdissection (PixCell II LCM, Arcturus).The tissue genetic identity was determined by using either the PowerPlex 16 ® multiplex (Promega), an assay based on short tandem repeat (STR) polymorphism in nuclear DNA (15 autosomal loci and the Amel locus on X/Y chromosome), or the Linear Array mtDNA HVI/HVII Region Sequence Typing kit (Roche Molecular Systems) for the mitochondrial DNA (mtDNA), in cases with insufficient nuclear DNA/negative STR data. The mtDNA test is based on sequence specific oligonucleotide probe analysis of hypervariable mtDNA d-loop regions I /II, and yields results for extracts containing less than 1pg of nuclear DNA. The samples underwent standard extraction and DNA quantitation (QuantiBlot).

Results: In all cases the identity of the tissue in question was established by either PowerPlex16® (7 cases), or mtDNA (6 cases) in case with inadequate nuclear DNA. Even though mtDNA types are not unique and shared by all maternal relatives, the discriminative power was sufficient to show exclusions of possible tissue sources.

Conclusions: The combination of multiplex STR and linear array mtDNA used in forensic investigation proved to be effective in a clinical laboratory, and may serve as a QA tool.

1518 Quantitative Determination of Neutrophil Morphologic Changes by Coulter Automated Hematology Analyzer with VCS Technology

F Chaves, B Tierno, S Smith, D Xu. Boston Medical Center, Boston, MA.

Background: Morphologic changes of neutrophils in response to cytokine stimulation during acute infection include toxic granulation, toxic vacuolization and Dohle bodies. The shortened transition of reactive neutrophils results in increasing bands and metamyelocytes (left shift). However, identification of these morphologic changes traditionally requires manual examination of peripheral blood smears, which is labor-intensive and subjective. Using the Coulter automated hematology analyzer (Coulter LH 750) with VCS technology, more than 8000 leukocytes can be directly analyzed using direct current impedance for cell volume (V), radio frequency opacity for conductivity (C) and a laser beam to measure light scatter (S) for cytoplasmic granularity and nuclear structure. Since left-shifted reactive neutrophils are larger and have lower nuclear complexity than their resting counterparts, we hypothesize that such morphologic changes may be quantitatively measured using the Coulter LH 750.

Design: We retrospectively analyzed data from septic patients with positive blood cultures (N= 69; M/F=36/33; mean age=52). Patients whose blood cultures yielded bacteria likely to be contaminants, such as coagulase negative Staphylococci, were excluded from the study. The controls (N= 33; M/F=10/23; mean age=51) were selected from patients whose complete blood count and differential data were within normal limits and had no signs of infection. VCS parameters of neutrophils, which are generated by each individual cell passing through the aperture, and optically and electronically measured by Coulter LH 750, reflect the mean channel numbers of cell volume (V-MCN), cell conductivity (C-MCN), and light scatter (S-MCN). Statistical analysis was performed using Student t test.

Results: A significant increase in V-MCN was observed in the neutrophils from the septic patients compared to controls (156 ± 13 versus 143 ± 4; $p < 0.001$). On the other hand, S-MCN was significantly decreased in patients (140 ± 10 versus 146 ± 7; $p = 0.001$), indicating left shift transition. No difference was observed in C-MCN between these two groups (141 ± 4 versus 142 ± 3; $p = 0.08$).

Conclusions: We demonstrated that the Coulter LH 750 could quantitatively measure morphologic changes in reactive neutrophils. We showed that reactive neutrophils from septic patients have significantly higher V-MCN and lower S-MCN. We believe that both V-MCN and S-MCN may be used as an additional indicator for acute infection.

1519 Detection of Microscopic FOCI of Metastatic Melanoma in Sentinel Lymph Nodes

AW Davis, A Palekar, K Schoedel, UN Rao. University of Pittsburgh Medical Center, Pittsburgh, PA.

Background: Sentinel lymph node (SLN) dissection has become a standard component of melanoma staging. Completion lymph node dissection (CD) is performed if metastasis is identified. It is of vital importance to identify melanoma in SLNs. Microscopic metastases may be difficult to visualize by routine stains. Melanophages may also hinder accurate diagnosis. Immunohistochemical (IHC) stains using several melanoma markers are often useful. SLN dissections were performed on 549 patients at our institution from 1996-2003. Of these, 67 patients had metastatic melanoma in SLNs.

Design: SLNs were subject to a standardized protocol in which they were bisected and 18 serial sections prepared. IHC stains with S100, MelanA, HMB45, and CD68 were performed using a red chromogen. Tyrosinase was later added to the panel. For this study, all positive SLNs and completion dissections were reviewed independently by 4 pathologists. IHC results were recorded and tabulated. Sensitivities and specificities of the IHC stains were statistically analyzed.

Results: 44 patients had SLN dissections that included more than one lymph node. 170 SLNs were evaluated in 67 patients. 70/170 lymph nodes were positive for metastatic melanoma. In 4/70 positive SLNs, tumor was detected by IHC stains only. In 39/70 positive SLNs, S100, MelanA, and HMB45 were performed in combination. In 38 of these cases, CD68 was also performed. In 11/70, S100, MelanA, HMB45, and tyrosinase were performed. In all cases, melanoma was negative for CD68. S100 sensitivity was 100% (95% confidence interval (CI) 91-100%) with specificity of 97% (95% CI 88 - 99%). S100 positive dendritic cells were typically easily distinguished from melanoma by morphology. MelanA sensitivity was 79% (95% CI 63-90%) with specificity of 94% (95% CI 79-99%). HMB45 sensitivity was 81% (95% CI 67-91) with specificity of 98% (95% CI 90-100). The number of tyrosinase cases was too small for statistical analysis. Additional lymph nodes contained tumor in 12% of CD.

Conclusions: S100 is highly sensitive and specific for identification of microscopic melanoma in SLNs when combined with morphologic features and serial sections. HMB45 and MelanA have lower sensitivities than S100, but improve overall efficacy of the IHC panel. Melanoma cells were negative for CD68 in all cases, and CD 68 was useful for identifying melanophages.

1520 Slide Based, Whole Cell Her2neu FISH Amplification: Mechanisms of Expression and Correlation with Immunohistochemistry

SA Dayan, JF Silverman, YL Liu, CA Smith, SE Shackney. Allegheny General Hospital, Pittsburgh, PA.

Background: Previous studies suggest there are several distinct genetic mechanisms that produce increased Her2/neu gene copy per cell including aneuploidy, Her2neu amplification in the absence of aneusomy (aneuploidy) and a combination of gene amplification and aneuploidy. We evaluated slide based, whole cell amplification for Her2/neu by FISH, a method that minimizes signal loss due to partial sectioning and correlated the results with protein expression by immunohistochemistry (IHC), scored by the Hercep Test protocol.

Design: Resected breast carcinomas from 72 women ranging in age from 34-85 years old (mean 55.5 y/o) were analyzed. The series consisted of 69 invasive ductal carcinomas including 4 with a lobular component and 2 with a papillary component, along with 2 metaplastic carcinomas and 1 invasive lobular carcinoma. FISH studies were done on slide base, whole cells in smears. FISH was performed by Vysis using gene specific probes for Her2/neu/chromosome 17. Amplification was defined by more that 15% of the cells having a greater gene copy number than chromosome copy number. Aneuploidy was determined by centromere counts. IHC for Her2/neu was performed using the Dako antibody and Hercep Test scoring system (DAKO, Capinteria, CA). Statistical analysis employed was students T-test and Chi-square.

Results: The results are shown in the table:

FISH/IHC Correlation

IHC	No.	Diploid	Aneuploid	Amplified
Total	72	35	17	20
Score 0	26	20	2	4
Score 1	16	6	5	5
Score 2	16	5	7	4
Score 3	14	4	3	7

Conclusions: • Her2/neu amplification by FISH is due to aneuploidy (increase chromosome copy number) and/or increase gene copy number/cell as determined by slide based, whole cell analysis.

• 50% of breast carcinomas with no FISH amplification as determined by increased gene copy or excess chromosome copy numbers in whole cells were IHC score 3, with possible overtreatment implications with trastuzumab (Herceptin).

• 9/42 (31%) of negative IHC score (0 and 1+) demonstrated FISH amplification, with undertreatment implications.

• These results may reflect a greater sensitivity of FISH using slide based, whole cell technique, compared to conventional FISH performed on histology based, partially sectioned preparations.

1521 Balancing Education and Turnaround Time: The University of Iowa Experience with Implementation of Rapid Continuous Tissue Processing

BR DeYoung, MB Cohen. The University of Iowa, Iowa City, IA.

Background: Maintaining balance between providing sufficient time for education and responding to pressures for improved specimen turn around time is difficult. The advent of rapid continuous tissue processing (RCTP) has made "same day sign-out" possible and is desirable from both hospital administrators' as well as patients' perspectives. This "advance", however, may not be entirely compatible with an academic medical center's educational mission. Beginning in April of 2004, RCTP was implemented with the stated goals of improving specimen turn around time while maintaining the quality of our educational program.

Design: Three primary variables were identified with a comparison made between the months of March (pre-RCTP) and August 2004. The variables included turn around time (accessioning to sign-out (A to SO) and accessioning to hot seat (A to HS)), slide quality, and quality of educational experience measured by resident satisfaction compared to pre-implementation and time available for resident preview of slides prior to sign-out.

Results: The initial schemes designed to achieve the goals underwent significant modification in the time immediately following implementation. Once an workable system was in place, trends were as follows: mean A to SO time decreased from 29 to 21

hours and mean A to HS time decreased from 26 hours to 19 hours. The number of cases delivered to the HS within 12 hours increased 50 fold. Slides showed a greater degree of variability in quality and an occasional specimen showed "homogenization" artifact at their periphery. After redesign of the sign out schedule multiple times, specimens were placed on a two-day system while residents rotated on a three-day cycle. This resulted in resident satisfaction similar to pre-RCTP and no appreciable change in time allotted for slide preview.

Conclusions: While the process continues to evolve, the data suggests that an academic center can successfully implement RCTP in response to increasing pressure for more rapid specimen turn around while simultaneously maintaining the quality/integrity of educational programs.

1522 CD117 Immunohistochemistry Tissue Microarray for Quality Assurance and Inter-Laboratory Comparison: A CAP Cell Markers Committee Study

DM Dorfman, MM Bui, RR Tubbs, ED Hsi, AR Cohen, PL Fitzgibbons, MD Linden, RR Rickert, PC Roche. College of American Pathologists, Northfield, IL.

Background: We have developed tissue microarray-based surveys to allow a large number of laboratories to compare their performance in staining predictive immunohistochemical markers, including CD117 (c-kit), a protooncogene that is characteristically expressed in gastrointestinal stromal tumors (GISTs). GISTs exhibit activating mutations in the c-kit protooncogene rendering them amenable to treatment with Imatinib mesylate, a c-kit-selective tyrosine kinase inhibitor. Consequently, correct identification of CD117 staining is important for the diagnosis and management of GISTs.

Technology and Design: We contructed tissue arrays of tumor core samples, which were used to generate hundreds of tissue sections sufficient for large-scale inter-laboratory comparison of immunohistochemical staining.

Results: An initial 10 tissue core microarray survey of 63 laboratories, consisted of cores of GIST (4 cases), uterine leiomyoma (1 case), peripheral nerve sheath tumor (1 case), uterine stromal sarcoma (2 cases), and leiomyosarcoma (2 cases). Using polyclonal (85%) or monoclonal (15%) anti-CD117 antibodies, automated (94%) or manual (6%) immunostaining, and various antigen retrieval methods, participants achieved >80% staining concordance for 7 of 10 cores, including all 4 CD117-positive GIST cases. Discordant staining in 3 cores was likely due to the presence of necrotic foci in 1 core or CD117-positive mast cells in 2 cores.

Conclusions: There was good performance among a large number of laboratories performing CD117 immunohistochemical staining. Tissue microarrays for CD117 and other predictive markers should be useful for inter-laboratory comparisons and quality assurance.

1523 BRCA1 and BRCA2 Mutation Screening Using High Resolution Melt Curve Analysis

SD Dufresne, DR Belloni, OA Adeyi, WA Wells, GJ Tsongalis. Dartmouth-Hitchcock Medical Center, Lebanon, NH.

Background: Mutations in BRCA1 and BRCA2 greatly increase the risk of developing both breast and ovarian cancer and are responsible for approximately 80% of inherited breast cancers. In the Ashkenazi Jewish population, one of three mutations (185delAG or 5382incC in BRCA1 and 6174delT in BRCA2) are present in over two percent of individuals. It is important to identify patients who carry these mutations so that they can receive early screening for breast cancer and can be considered for prophylactic oopherectomy. Current methods for identifying these mutations are time consuming since they involve either DNA sequencing or gel electrophoresis after PCR amplification of the genes. In this study we developed a fast and reliable method to screen for the three most common BRCA1 and BRCA2 mutations in the Ashkenazi Jewish population using high resolution melt curve analysis.

Design: Primers were designed to amplify the regions in which these three common mutations are found. Real time PCR utilizing SYBR Green was then used to amplify DNA samples from cell lines known to carry either the 185delAG or 5382insC mutation in BRCA1 or the 6174delT in BRCA2. After amplification, the T_m and the shape of the melt derivative curves were analyzed for differences between wild type and mutant alleles.

Results: Significant differences were present in the melt curves for each of the mutations compared to those of the wild type sequences. For both the 185delAG and 6174delT mutations the melt curve derivatives had a shoulder at a lower temperature representing melting of the heteroduplexes. The melt curve for the 5382insC mutation was shifted to the right and was broader than the melting curve of the wild type sequences.

Conclusions: High resolution melt curve analysis is a quick, reliable method for identifying the three most common mutations in BRCA1 and BRCA2 in the Ashkenazi Jewish population. This technique can detect a one base pair difference in PCR amplified product and would eliminate the need for DNA sequencing or electrophoresis.

1524 Cocktail of Epithelial Markers Increases the Diagnostic Sensitivity for Sarcomatoid Carcinoma

YM EL-Gohary, X Lin, RS Saad, M Tung, YL Liu, JF Silverman. Allegheny General Hospital, Pittsburgh, PA.

Background: Sarcomatoid carcinomas are uncommon, aggressive malignancies occuring in various organs. Separation from sarcoma is important and can be difficult on histology due to their similar cytomorphologic features. Immunohistochemical (IHC) studies for various epithelial and mesenchymal markers are often performed to establish the correct diagnosis. However, the mesenchymal component of sarcomatoid carcinoma can be negative or very focally positive for epithelial IHC markers. We investigate whether an epithelial cocktail immunostain can better confirm the epithelial nature of a sarcomatoid carcinoma.

Design: 20 cases of sarcomatoid carcinomas of various sites were retrieved from the hospital computer. 15 cases of sacomatoid carcinoma had a histologic malignant epithelial component. 12 cases of sarcomas were included in the control group. Epithelial markers CAM 5.2, EMA, AE1/AE3, CK5/6, CEA, K903, and a cocktail of cytokeratins consisting of CAM 5.2 and CK5/6, along with EMA were performed using an automated immunostainer with appropriate positive and negative controls.

Results: Cytokeratin cocktail immunoreactivity was seen in the malignant spindle cell component of 90%(18/20) sarcomatoid carcinomas. CAM 5.2 was positive in 80% of the sarcomatoid carcinoma. EMA immunoreactivity was observed in 70% of the cases and was positive in one case which was negative for CAM 5.2. CK5/6 and K903 were also positive in a case which was negative for CAM 5.2.

Immunohistochemical findings

	Cocktail	CAM 5.2	EMA	AE1/AE3	CK5/6	CEA	K903
Sarcomatoid carinomas	18/20 (90%)	16/20 (80%)	14/20 (70%)	14/20 (70%)	10/20 (50%)	8/20 (40%)	10/20 (50%)
Sarcomas	2/12 (16.7%)	2/12 (16.7%)	0/12 (0%)	0/12 (0%)	0/12 (0%)	0/12 (0%)	0/12 (0%)

Conclusions: Our results indicate that a cocktail of CAM 5.2, EMA and CK5/6 can increase the detection of epithelial differentiation in sarcomatoid carcinoma and has greater sensitivity than using a limited number of individual epithelial markers.

1525 Multiple Displacement Amplification and the Detection of Human Papillomavirus (HPV) Physical State

MF Evans, CS-C Adamson, GM von Walstrom, K Cooper. University of Vermont, Burlington, VT.

Background: Multiple Displacement Amplification (MDA) is a new technique for whole genome amplification. From as little as 10ng of sample DNA more than 40µg of amplified product can be obtained. The method utilizes Phi29 DNA polymerase that has a high proofreading capacity, and which also has high processivity allowing the amplification of DNA up to 70 kilobase pairs. An inherent 'strand displacement' property allows the polymerase to amplify DNA without the need for thermal cycling. Since the method synthesizes large quantities of DNA from small starting amounts, MDA may also be useful in pathology research and diagnosis where patient tissue sample availability is limiting. In this study MDA has been examined as a potential aid for examining HPV integration in cervical tissues.

Design: Validation experiments have been conducted to confirm the technique accurately represents the HPV genome. Firstly HPV/recombinant plasmids (HPV-types 6, 16, 18, 31, 43, 45) were amplified by MDA. Restriction fragment patterns after digestion of original plasmid samples and MDA products with *BamH*I, *Cfr*I, *Eco*RI, *Hae*III, *Hind*III, or *Pst*I were compared. Secondly, the *E1*, *E6/E7*, and *LCR* regions of HPV-16 were sequenced from the plasmid and MDA products. Thirdly, DNA from cervical cell lines containing integrated HPV (CaSki, SiHa [HPV-16 positive], and HeLa [HPV-18 positive]) were amplified by MDA. These samples and DNA extracted directly from the cell lines were restricted with *BamH*I, *Eco*RI, *Hind*III, *Hpa*II, *Kpn*I, *Msp*I, *Pst*I, or *Xho*II and HPV Southern blot hybridization patterns were compared. In addition the HPV-16 *E6/E7* sequences from CaSki and SiHa cell DNA were compared with the same sequences obtained after MDA.

Results: Comparing MDA products and the original DNA templates, identical restriction fragment patterns were obtained from HPV/plasmid recombinants and from cell lines except when methylation sensitive (*Cfr*I, *Hpa*II) restriction enzymes were used. In these instances significantly different band patterns were evident. Sequencing analyses demonstrated that the MDA technique accurately copied sequences from plasmid HPV and integrated cell line HPV.

Conclusions: These model data demonstrate that the MDA technique can be used to investigate HPV integration and support the possibility that DNA extracted from limiting quantities of cervical biopsy or Pap smear samples and amplified by MDA could be suitable for HPV physical status assay. The data also suggest the possibility MDA may be used in investigations of DNA methylation status.

1526 Paraffin Embedded Cell Lines Microarray (PECLIMA): A High-Throughput Method for Antigen Profiling of Cell Lines

B Ferrer, R Bermudo, TM Thomson, J Calvo, M Soler, I Nayach, M Sanchez, E Campo, PL Fernandez. Hospital Clinico-IDIBAPS- Universidad de Barcelona, Barcelona, Spain; CSIC, Barcelona, Spain.

Background: High-throughput techniques are increasingly providing abundant information on molecular alterations requiring validation at the postranscriptional level. Protein expression is now efficiently evaluated in large series of tumors included in tissue microarrays. We here propose, describe and validate a technique to ellaborate paraffin embedded cell lines microarrays (PECLIMA) from fixed cell cultures, which can be processed like standard surgical pathology biopsies prior to immunophenotyping.

Design: PECLIMAs were developed using several human cancer cell lines: LNCaP, PC3, DU-145, RWPE1 and RWPE2 and HeLa. Agar was used for the generation of cell line plugs. Generated paraffin blocks provided the cores to construct PECLIMAs using a tissue microarrayer. The arrays contained cell lines fixed in 10% formalin for 5 minutes and 2 hours as well as in 4% paraformaldehide for 5 minutes. The expression of different antibodies was evaluated by immunocytochemistry in the three different fixation conditions, and included: CAM 5.2, AE1-AE3, 34betaE12, Keratins cocktail, Ker5, Ker7, Ker20, PSA, chromogranin, NSE, synaptophisin, P53, P27, ER,PR, AR, Ki-67. Selected antibodies were used in fluorescence immunocytochemistry for validation. FISH was also performed on the PECLIMA sections using the PathVysion Kit.

Results: The expression profiles of the cell lines were highly consistent in the different fixation conditions. Ker5, Ki-67 and Ker7 were positive in all cell lines and in all fixation conditions, whereas NSE, CHG, ER and PR were completely negative in all cell lines and in all fixation conditions. In general, similar results were obtained for five minutes fixation with formalin and paraformaldehyde. The majority of the antibodies were better detected with 5 minutes than 2 hours formalin fixation. There was good concordance between the results observed for PECLIMA and immunofluorescence on coverslips.All cell lines on PECLIMA showed adequate resistance to the FISH processing protocol as well as hybridization signals.
Conclusions: We conclude that the TMA technic is suitable for fixed cell lines and improved by the use of agar to manipulate the cell pellets, while preserving an adequate morphology and immunophenotype of the cells. We therefore consider the PECLIMA method as a powerful ally for high-throughput phenotypic evaluation of cell lines.

1527 High-Throughput Automated Image Analysis of Multitarget Fluorescence In Situ Hybridization (FISH) Assay in Patients with Bladder Cancer and Atypical or Negative Urine Cytology

JL Fine, E Swain, RR Tubbs, J Pettay, M Hartke, K Keslar, K Simmerman, M Skacel. Cleveland Clinic Foundation, Cleveland, OH.
Background: Urothelial carcinoma (UC) is an important cause of mortality and morbidity. Multitarget fluorescence in situ hybridization (FISH) of urine cytologic specimens for abnormalities of chromosomes 3, 7, 17 and 9p21 locus is a highly sensitive and specific test for the detection of UC (UroVysion, Vysis, Downers Grove, Illinois). Interpretation of this test is labor intensive and involves manual evaluation of four FISH probes in each case, utilizing oil-immersion microscopy. A high-throughput, automated image analysis system would permit fast and accurate scoring of this test.
Design: Nine urine cytology specimens were examined (ThinPrep, Cytic, Boxborough, MA). The UroVysion test was performed, and the cases were scored manually by three experienced technologists using FDA-approved guidelines to establish a positive result. The cases were then scanned and analyzed by a high-throughput automated image analysis system (MetaSystems, Altlussheim, Germany). The system was trained to recognize single cells, and to correctly recognize discrete probe signals in four colors. The manual and automated interpretations were compared.
Results: There was good overall agreement between manual and automated results. Sensitivity was excellent, as the system correctly identified all positive cases (5 of 9 total cases). The system correctly identified half of the negative cases (4 of 9 total cases). Discrepant results were caused by the variability in signal intensity and size of each of the probe signals, as well as occasional over-interpretation of split signals. Adjustment of the image analysis classifiers significantly reduced the susceptibility of the system to these errors.
Conclusions: High-throughput image analysis is a promising automated alternative for the interpretation of the UroVysion test for UC detection in urine cytology samples. Further refinement of classifiers will rapidly improve the accuracy of the automated scoring and reduce the need for labor-intensive manual scoring. Future studies of a larger series will be necessary to validate this application for routine clinical use, thereby reducing labor requirements inherent to this increasingly utilized test.

1528 Quantitative ELISA-Like IHC (QUELI) on FFPE Tissue

C Genty, S Mao, SK Mohsin, DC Allred. Baylor College of Medicine, Houston, TX.
Background: The majority (>99%) of human tissues are stored as FFPE blocks. Measuring proteins in FFPE samples is primarily restricted to IHC, which is good at identifying the source but poor at quantification. In contrast, the ELISA is poor at identifying the source but good at quantifying. We combined IHC and ELISA into a new assay (QUELI) which can determine the source and quantity of multiple proteins simultaneously in intact FFPE tissue.
Design: As a demonstration, 3 µm serial sections from a 2 mm core of FFPE tonsil were placed into water-filled wells of a 96-well microarray plate. Sections adhered to the bottom following evaporation. They were deparaffinized and subjected to epitope unmasking in a thermocycler at 110° C. Thereafter, the plate was subjected to a series of reagents and washes following a standard ELISA-like procedure. At the primary antibody step, each of 24 different antibodies was plated into 4 consecutive wells. At the chromogen step, the first well received an insoluble chromogen (H_2O_2/DAB) and the remaining three received a soluble chromogen (H_2O_2/TMB) which was allowed to react for 30 minutes. The sections with DAB were visualized microscopically. The sections with TMB were quantified by measuring optical density (OD) with a microplate reader.
Results:
Source (% pos cells) and quantity (OD) of 24 proteins.

Antibody	% Pos Cells	Avg OD (Triplicate)	P-Value (vs. Neg)
Neg Mouse (M)	0%	0.069	NA
Neg Rabbit (R)	0%	0.022	NA
P53 (M)	<1%	0.196	<.0001
IgA (R)	1%	0.200	<.0001
Leu-M1 (M)	5%	0.251	<.0001
Mac387 (M)	5%	0.323	.0001
IgM (M)	5%	0.379	.0006
Caspase 3 (R)	1%	0.383	<.0001
Mitosin (M)	5%	0.416	<.0001
KP1 (M)	5%	0.505	<.0001
Lambda (R)	10%	0.630	<.0001
Topoisomerase II (M)	5%	0.694	<.0001
IgG (R)	10%	0.935	.0004
P27 (M)	75%	1.510	<.0001
CD31 (M)	10%	1.596	<.0001
Kappa (R)	15%	1.672	.0002
Cytokeratin (M)	5%	1.760	<.0001
MIB1 (M)	20%	1.932	.0003
Bcl2 (M)	80%	1.993	.0001
Tubulin (M)	25%	2.219	<.0001
CD3 (R)	40%	2.743	<.0001
CD45 (M)	95%	3.019	<.0001
CD20 (M)	60%	3.457	<.0001

Conclusions: QUELI is an easy and inexpensive method to determine the source and quantity of multiple proteins simultaneously in intact FFPE tissue, and may be a useful tool for clinical research.

1529 Analytic Validation of Molecular Analysis of Pancreaticobiliary Brushing Cytology Specimens

OE Gologan, S Finkelstein, O Lapkus, YL Liu, PA Swalsky, M Wilson, JF Silverman. Allegheny General Hospital, Pittsburgh, PA; Redpath Integrated Pathology, Pittsburgh, PA.
Background: The integration of molecular analysis into cytology practice has the potential to reduce indeterminate diagnosis and facilitate the earlier detection of cancer at a time when morphologic changes may not be easily discerned. To accomplish this integration, the reliability of molecular analysis must be assessed on an individual case basis. We sought to define conditions that would best enable analytic validation of mutational analysis to be performed in the context of cytology analysis.
Design: Eighteen (18) pancreatic and fifteen (15) biliary brush cytology specimens were gathered from cytology archives of a tertiary, academic medical center (1999-2004). Xylene resistant markings were placed on the slide underslide and coverslips removed. Clusters of normal, atypical and malignant appearing stained cells were manually microdissected into two equivalent collections of samples for mutational analysis. The microdissection technique ensured that topographic distribution of cells into each independent collection was similar. DNA was extracted and mutations (allelic imbalance [LOH]) were quantitatively determined for a broad panel of 15 molecular markers (1p,3p,5q,9p,10q,17p,17q,21q,22q) as well as point mutation in k-ras-2 using PCR/capillary electrophoresis. The presence, cumulative amount and time course of mutational damage was correlative between the two topographically equivalent sample collections (intraclass correlation coefficient of reliability)
Results: Duplicate microdissection provided 288 individual pancreatic mutations analysis of which 275 (95%) were strictly concordant. 164 of 168 bile duct duplicate analysis were concordant (98%). Of 17 instances of difference, 15 involved mutations in which 70% or less of microdissected cells were altered thereby reflecting late acquired mutations. Only 2 instances (less than 1%) involved early acquired mutations. 92% and 95% of patient pancreatic and biliary genotyping profiles were concordant respectively including 20 overall in which the complete 16-marker panel matched perfectly.
Conclusions: A simple and effective means to ensure analytic accuracy in molecular cytology analysis is to require that the mutational profiling be carried out on two equivalently microdissected yet independent cellular samples. The selection should reflect the most representative cellular targets selected according to cytomorphologic features.

1530 Epidermal Growth Factor Receptor (EGFR) Expression in Colorectal Carcinoma: Image Cytometric Quantitation

M Gupta, G Costonis, D Lawson, C Cohen. Emory University School of Medicine, Atlanta, GA; Emory University School of Public Health, Atlanta, GA.
Background: Epidermal growth factor receptor (EGFR) is implicated in malignant cell proliferation and cancer progression.Cetuximab (Erbitux), a chimeric human-mouse-monoclonal immunoglobulin G1 antibody, is used alone or in combination with Irinotecan, for the treatment of EGFR-expressing, metastatic colorectal carcinoma that has progressed following chemotherapy. Over 20% of patients respond to the combination, predicted by EGFR expression in the carcinoma. This study compares visual estimation of EGFR expression to image cytometric quantitation in colorectal carcinoma.
Design: Thirty-one (27 primary, 4 metastatic) colorectal carcinoma were immunostained with EGFR monoclonal antibody (DakoCytomation: Clone 2-18C9) (DAKO).Results were visually assessed by two authors as intensity (0-3+) and scored according to estimated percentage of cells with membranous immunostain (0=negative, 1=1%, 2=2-5%, 3=6-10%, 4=11-25%, 5=26-50%, 6=51-75%, 7=76-100%). Membranous immunostain was also quantitated by image cytometry (0-3+) using the Ariol SL-50 (Applied Imaging, San Jose, CA) subcellular analysis within cell compartments, rather than stain intensity values. Results by both methods were compared.

Results: Visually, 25 (80.7%) of carcinomas expressed EGFR. In 92%, this was of 2+ and 3+ intensity. More than 25% of carcinoma cells (scores 5-7) were immunopositive in 72%; 28% had 6-25% EGFR-expressing cells (scores 3 and 4). By image cytometry, 96.8% (30 of 31 cancers) were EGFR-positive; 80% scored 1 and 20% 2. There was concordance between EGFR-positive cases by the two quantitative methods in 77.4% (24 of 31). The 7 (22.6%) discordant cases included 6 negative by visual assessment but quantitated as 1 (5) and 2(1) by image cytometry. The seventh discordant case (3+intensity,score 7) was negative by image cytometry. Chi-square and Fisher's Exact Test showed no significant difference ($p>0.05$) between the results obtained by the two methods of quantitation.

Conclusions: Image cytometric analysis of membranous EGFR immunostain is an easy, quick, objective technique to assess predictability of response to erbitux in patients with metastatic colorectal cancer. Seventy seven percent of results are concordant with those by visual assessment. Eighty five percent of discordance is due to negative visual assessment but scores of 1 and 2 by image cytometry, indicative of the greater sensitivity of image analysis.

1531 Proteomic Evaluation of Breast Neoplasm Fine-Needle Aspirations by SELDI-TOF: Comparison of PreservCyt® Versus Fresh-Frozen in Buffered Saline Methodology

JL Herrick, LJ Fowler, I-T Yeh, D Campos, E Izbicka. UTHSCSA, San Antonio, TX; CTRC, San Antonio, TX.

Background: Proteomic profiles of tumor protein expression by the SELDI-TOF methodology have been shown to be a new ancillary technique potentially useful for diagnosis, prognosis and therapeutic considerations of cancer from several organ systems. Fine-needle aspiration (FNA) specimens from tumor samples are an accepted method for diagnosis but occasionally may only allow limited assessment. The current pilot study compares SELDI-TOF protein pattern preservation in a range of breast tumors collected by FNA and placed concurrently in PreservCyt® (PC) and buffered normal saline with snap freezing (BNS-SF).

Design: Excised fresh breast tissue from a variety of breast lesions were sampled by FNA and placed into PC for storage at room temperature up to 6 weeks, or in BNS-SF and stored at -70° C. Both BNS-SF and PC samples were centrifuged and washed in phosphate buffered saline. Small pellets were homogenized on ice in 100 µl urea/CHAPS buffer with protease and phosphatase inhibitors, clear lysates collected by centrifugation, and stored in small aliquots at -80°C. Protein concentration was measured by BCA assay (Pierce). SELDI-TOF analysis on diluted samples was performed in duplicate on metal affinity IMAC-3/Cu ProteinChip arrays with appropriate quality control assays. Sample handling was accomplished in a Biomek2000 robotic workstation (Beckman Coulter) in a 96-well bioprocessor. Arrays were analyzed in PBS-IIC reader (Ciphergen Biosystems).

Results: Extracts from BNS-SF and PC-stored specimens showed a broad range of protein concentrations. Preliminary analysis of proteomic profiling of 15 benign cases (fibroadenoma) and 15 malignant lesions (ductal carcinoma in situ and ductal carcinoma) revealed similar patterns in both types of preparations. When 8 matched specimens at similar protein concentrations were analyzed, the proteomic complexity (number of peaks) was comparable in the BNS-SF preparations versus the same tissue placed in PC.

Conclusions: FNA of breast tissue placed in PC is an acceptable method of sample handling for evaluation by the SELDI-TOF methodology to aid in ancillary cytology diagnosis. Further comparative studies on PC storage versus fresh/frozen methodology are warranted to determine if PC storage is compatible with further protein characterization. Our results from benign and malignant breast lesions support SELDI-TOF's strong potential for ancillary testing in the evaluation of breast cancer by FNA.

1532 Telepathology: Three Years of Routine Evaluation of Breast Lesions

CL Hitchcock, LE Hitchcock, S Suster. The Ohio State University, Columbus, OH.

Background: Telepathology is a cost effective means of providing effective pathology service. This study reviews the results of three years of experience using telepathology to provide routine gross and microscopic assessment of breast lesions in support of a free-standing surgical center.

Design: A dynamic telepathology (TP) system (MedMicro, Trestle, Corp) was established at a breast cancer center located 11 miles from the main campus hospital. The system consists of an Olympus BX50 microscope (2,4,10,20, 60x) equipped with a x,y,z motorized stage (Prior), an Olympus PMTV camera, digitizer (Imaging Technology), and macro stand equipped with an Olympus PMTV camera. Signals are transmitted over a T3 line to the desk of each pathologist. During 3 year period, 314 breast tissue specimens were submitted, and processed by an on-site technologist for TP. Pathologists reviewed an image of the gross specimen and decided whether or not a specific area was to be sampled for a frozen section (FS). Each FS was H and E stained. Each TP diagnosis (TPDx) was compared with to the final tissue diagnosis (FTDx).

Results: No frozen section was obtained in 117 of 314 biopsies (37.3%) due to: gross only diagnosis (23), no distinct lesion to sample (75), lesion < 1 cm (17), and FS not performed (3). Resulting FTDx of a malignancy was associated with sampling error (DCIS: 3 cases), cryostat malfunction (ductal carcinoma: 1 case), and lesion <1cm (LCIS: 1 case, ductal carcinoma: 2 cases). A total of 191 TPDx were made and 6 cases were deferred. For the 191 cases submitted for FS there was 96.3% (184/191) concordance between TPDx and FTDx for benign and malignant lesions. Discordance was due to sampling (3 cases) and a TPDx of atypical cells (4 cases). Concordance rates for FS slides examined by TP and final review were 98% intra-observer (149/152) and 97% (32/33) intra-observer.

Conclusions: Dynamic telepathology allows the pathologist to provide an accurate gross and microscopic assessment of frozen sections of breast lesions. Integration of telepathology into the routine flow of surgical pathology requires close attention to system errors.

1533 Tissues Fixed in Stabilization Solution 'RNAlater' - Effect on Immunohistochemistry

AA Jungbluth, D Kolb, SK Eastlake-Wade, KJ Busam, DB Flieder. Ludwig Institute for Cancer Research, New York, NY; Memorial Sloan-Kettering Cancer Ctr., New York, NY; Fox Chase Cancer Ctr., Philadelphia, PA.

Background: There is a great need for tissue fixation procedures allowing downstream applications such as RT-PCR and IHC on the same specimen. 'RNAlater' is a commonly used commercially available solution for the preservation of RNA in fresh tissue samples without the need for freezing procedures. Previous analysis suggested that morphology and IHC are unaffected by RNAlater fixation. However, we observed altered IHC expression of several antigens after RNAlater fixation. Consequently, the present study analyzes the effect of RNAlater fixation on IHC.

Design: 34 lung and esophageal tumors were analyzed. Tissue pieces of the recommended size were fixed in 'RNAlater' (Ambion) immediately after surgical removal for 3 to 6 hrs. Specimens were then transferred to 10% NBF and processed into standard paraffin blocks and subsequently analyzed by IHC for the following mAbs (antigens): MA454 (MAGE-A1), M3H67 (MAGE-A4), 57B (MAGE-A4), S100 (S100), CAM5.2 (LMW-Ck), UCHL-1(CD45RO). For each case, corresponding standard FFPE blocks not fixed in RNAlater were co-typed by IHC for the same mAbs/antigens.

Results: The morphology of tissues fixed in RNAlater was affected. In HE stains, nuclei often appeared glassy and nuclear borders were blurry. The size and shape of tumor cells appeared distorted, sometimes with spaces between cancer cells and surrounding stroma not present in the conventionally fixed tissues. The stroma appeared more homogeneous and gave a pinkish stain due to a reduced staining with hematoxylin. In IHC, several mAbs showed a reduced immunoreactivity in many tissues. Some cases which were immunopositive as conventional fixed tissues, were negative after RNAlater fixation. This was especially true for mAbs to the CT antigens MAGE. Though staining of cytokeratins and CD45RO was preserved in most cases, the immunopositive areas were blurry with indistinct borders; e.g. CD45RO positive cells only rarely revealed the typical membranous pattern.

Conclusions: RNAlater tissue fixation can alter morphology and IHC staining characteristics. In HE stains, this can lead to different morphological impressions and misleading interpretations. In IHC analysis, the antigen expression profile can be altered and in some cases eliminated. Great caution should be exercised using RNAlater solution for the fixation of tissues which are intended for immunohistochemical analysis.

1534 Clinical Validation of Immunoglobulin Gene Rearrangement Detection by PCR Using Commercially Available BIOMED-2 Primers

P Kaur, PJ Kurtin, EM Pagel, CE Lueck, PD Ouillette, RF McClure. Mayo Clinic, Rochester, MN.

Background: Polymerase chain reaction (PCR) – based assays are commonly used to detect clonal immunoglobulin (IG) gene rearrangements during the evaluation of lymphocyte infiltrates. Recently, an extensive set of PCR primers was developed by the European BIOMED-2 collaborative for use in such assays and the primers are now commercially available from InVivoScribe™ Technologies. Clinical validation of the primer sets for IG heavy and kappa light chains was performed.

Design: DNA from a total of 170 fresh or frozen samples was analyzed for the presence or absence of clonal IG gene rearrangements. Samples included normal tissue, reactive lymphoid hyperplasia and a variety of B-cell neoplasms. The BIOMED-2 primer sets for IG heavy and kappa light genes (a total of 34 upstream and 4 downstream primers) were used following the manufacturer's instructions with analysis on an ABI3100 genetic analyzer.

Results: See Table 1 for results summary.

Diagnostic sensitivity was 92% for non-Hodgkin lymphoma and 46% for Hodgkin lymphoma. Diagnostic specificity was 98%.

Conclusions: The BIOMED-2 primer sets evaluated have excellent diagnostic specificity and overall sensitivity for the detection of clonal IG gene rearrangements in fresh and frozen clinical specimens.

Table 1. Clonal IG Gene Rearrangement Detection Using BIOMED-2 Primers

Diagnosis *	Clone Detected
Normal	0/26 (0%)
Reactive lymphoid hyperplasia	1/29 (3%)
Angioimmunoblastic T-cell lymphoma	2/7 (29%)
B-cell chronic lymphocytic leukemia	20/20 (100%)
Mantle cell lymphoma	5/7 (71%)
Follicular lymphoma	27/29 (93%)
Marginal zone lymphoma	11/11 (100%)
Lymphoplasmacytic lymphoma	8/8 (100%)
Diffuse large B-cell lymphoma	16/20 (80%)
Classical Hodgkin lymphoma	5/12 (41%)
Nodular lymphocyte predominant Hodgkin lymphoma	1/1 (100%)

* Normal samples were blood and bone marrow; the remainder were frozen solid tissue

1535 Profiler: A Powerful Web-Based Tissue Microarray Analysis System and Relational Database for Collaborative Translational Research

R Kim, J Tang, S Lnu, R Shen, D Gibbs, V Mahavishnu, J Wei, CG Kleer, AM Chinnaiyan, MA Rubin. Brigham and Women's Hospital, Boston; Harvard Medical School, Boston; University of Michigan, Ann Arbor; Dana-Farber Cancer Institute, Boston.

Background: Tissue Microarrays (TMAs) allow for the evaluation of a large number of tissue samples stained by immunohistochemistry (IHC), in situ hybridization, or FISH on a single slide. Manual evaluations of TMAs limit flexibility and collaborative ability among researchers in regards to data collection. We present the continuing development of an Internet-based TMA profiling tool.

Design: TMA images are captured by BLISS® Slide Scanner (Bacus Laboratory Inc., Lombard, IL) and then transferred to the Profiler server currently based at 2 University sites. The Profiler system is a web-based application that allows remote access of the scanned images via the Internet. Each image is presented to the evaluator at high resolution, which can be viewed at several magnifications. The evaluator assigns a diagnosis to the core, ranks the staining intensity and assigns values to other parameters as applicable (Gleason Grade, Ellston-Ellis Grade, etc). The system has been in use since 2001.

Results: The design of Profiler's relational database makes it compatible with multiple organ system (e.g., prostate, breast, lung, renal, and hematopoietic system,). The system administrator can assign levels of access to evaluators using password protected profiles. For example, investigators at one institution cannot view studies or folder names from other groups. Data is protected by a secure Oracle relational database. The servers contains 585 scanned TMAs with 53,365 tissue samples. 66 pathologists from 12 major user groups including 8 S.P.O.R.E. groups use the system. 2 groups directly link clinical data from over 500 patients for immediate access. Profiler currently has 145K data points such as staining intensity, tumor grade, and nuclear size. Users can query their studies based on multiple parameters. The results are displayed as raw data and images. The system is also capable of inputting Chromavision data.

Conclusions: The implementation of Profiler into the research community creates the opportunity to centralize data and create an efficient work flow of TMA evaluations. Profiler facilitates collaborations among pathologists at different institutions. The Oracle-based server has all the required security tools to protect researcher-designated space allowing for multiple user groups on the same system.

1536 Application of Automated Standardized Immunohistochemistry in Formalin-Fixed Paraffin-Embedded Mouse Tissue for the Classification of Murine Lymphoid and Non-Lymphoid Hematopoietic Tumors

S Kunder, J Calzada-Wack, J Mueller, L Quintanilla-Martinez. GSF-Research Center for Health and Environment, Neuherberg bei Munich, Germany.

Background: The increasing importance of mouse models for the study of human diseases makes a standardized approach to the classification of murine neoplasms necessary. The recently proposed classification for murine hematopoietic tumors (Blood 2002, 100;238-258) recommends the use of immunohistochemistry (IHC) for the accurate classification of these neoplasms. However, most of the antibodies available are reactive only on frozen sections or useful for FACS analysis. The aim of this study was to establish a panel of antibodies useful for the diagnosis of lymphoid and non-lymphoid hematopoietic neoplasms in formalin-fixed paraffin-embedded mouse tissue.

Design: Paraffin-embedded tissue from 120 mice with lymphomas and leukemias were analyzed. Immunohistochemistry was performed on an automated immunostainer (Ventana Medical System) using the DAB and iView kits. Antigen retrieval was done in a microwave pressure cooker with citrate buffer pH 6.0 for 30 minutes. Thirty different antibodies (Abs) were analyzed, including monoclonal rat, monoclonal mouse, polyclonal rabbit and the new monoclonal rabbit Abs, covering a broad spectrum of lymphoid and myeloid antigens. Some Abs were raised against mice (B220), whereas many were crossreactive Abs primarily raised against humans.

Results: The following antibodies proved to be useful for the classification of murine hematopoietic neoplasias in paraffin-embedded tissue: 1) CD3, B220, CD79acyt, CD138, CD43, CD45, Tdt and Mac3 for lymphoid neoplasias. 2) myeloperoxidase and Ly-76 (TER-119) for myeloid tumors and erythroleukemia, and 3) Ki-67 (TEC-3) and p53 for both. The mouse reactive Abs cyclin D1, BCL-2, p27 and 21 were not contributory for the diagnosis of murine hematopoietic neoplasms. Specific staining for kappa, lambda and other immunoglobulins was not achieved. Monoclonal mouse and polyclonal rabbit antibodies gave the best staining with the DAB kit, as opposed to the iView kit, which gave a non-specific binding with the mouse immunoglobulins. The monoclonal rat and monoclonal rabbit antibodies showed specific staining with both kits.

Conclusions: In this study, we developed a comprehensive panel of antibodies in mouse formalin-fixed paraffin-embedded tissue useful for the classification of murine hematopoietic neoplasms. The application of IHC facilitates the analysis of these malignancies and the comparison with their human counterparts.

1537 Spectral Imaging for Automated Analysis of Multicolor Immunohistochemical Studies in Hematopathology

RM Levenson, C van der Loos, RC Braylan. CRI, Inc., Woburn, MA; Academical Medical Institute, Amsterdam, Netherlands; University of Florida, Gainesville, FL.

Background: Systems-based science and genomic advances have emphasized the need to understand biology and pathology in their full complexity. A fruitful approach is to use spatially resolved molecular probes to indicate where and when molecular events occur within cells and tissues. Simultaneous assessment of more than one analyte is desirable, and for maximum utility this should be achievable at the single-cell level. Fluorescence has traditionally been used for multiplexing, but there are advantages to non-fluorescent multicolor methods. This report describes the application of multispectral imaging for the spectroscopic "unmixing" of multiple chromogenic labels, with examples drawn from hematopathology.

Design: A variety of immunostained pathology samples were examined. Spectral datasets were acquired with one of two spectral imaging technologies: a CCD equipped with a liquid crystal tunable filter and mounted on a standard microscope C-mount; or a novel LED-based spectrally tunable light source that replaces the standard lamp at the rear of most microscopes. Spectral unmixing was performed using standard and customized spectral analysis tools, and quantitation of the unmixed results was performed using additional image analysis methodologies. Analyses of mature and immature thymus specimens for their CD4-CD8 phenotypes, and of post-treatment leukemic bone marrows for the presence of residual blasts were performed.

Results: Spectral unmixing could quantitatively recover the intensities of multiple chromogens even when they overlapped both spatially and spectrally. The transition from single positive to double positive CD4+/CD8+ thymocytes was easily demonstrated even when the individual antigens were labeled with DAB (brown) and Fast Red, a color combination that is difficult to unmix using conventional imaging approaches. Similarly definitive results were obtained with double-immunostained post-therapy leukemic bone marrow biopsies developed with brown and red chromogens for blast enumeration.

Conclusions: Spectral imaging allows the use of multiple chromogens for the immunophenotyping of hematopathology specimens and in certain situations can supplement or replace conventional immunofluorescence or flow cytometric studies while providing the convenience and ease of use of brightfield, chromogenic signals.

1538 Quantitative Assay of Hepatitis C Virus in Liver Biopsy Tissue

C Liu, C Soldevila, H Zhu, M Butera, R Forpi, A Hemming, DR Nelson. University of Florida, Gainesville, FL.

Background: Hepatitis C virus (HCV) an RNA virus that primarily infects human hepatocytes. Viral RNA is detectable in serum of the chronically infected patients. Several quantitative assays are available and routinely used in clinical practice. The serum viral load assays are widely used to monitor the interferon alpha-based therapy and viral infection recurrences in the setting of liver transplantation. However, little is known about the virological status in the liver tissue in these clinical settings. To determine the significance of viral load in liver tissue, we have developed a real-time PCR assay to quantitatively determine the levels of viral RNA in routine liver biopsy tissues.

Design: A fragment of liver core biopsy (0.5 cm) was collected from patients and immediately placed in RNAlater solution. Total cellular RNA was extracted from the liver tissue. The cDNA was generated using reverse transcriptase and served as the template for real-time PCR analysis. Lux™ primers were designed and synthesized in Invitrogen. One of the HCV primer was labeled with FAM, and one of the GADPH primer was labeled with JOE. Reactions were conducted in a 96-well spectrofluorometric thermal cycler (ABI PRISM 7700). Results from triplicate were represented as means ± SD and analyzed using SDS 2.0 software from Applied Biosystems. HCV viral standard curve was generated using in vitro transcribed full-length HCV-RNA genome. The serum viral load was obtained from a commercial laboratory. The correlation between the serum viral load and liver tissue viral load, and the clinical information were analyzed.

Results: HCV-RNA was detected in all the liver biopsy tissues from patents who had viral RNA in their serum (31/31, 100%, $p<0.001$), and the levels of viral RNA is comparable with serum viral load. Higher viral levels in the liver tissue were positively correlated with higher inflammatory grade. HCV RNA was present in five of eighteen (5/18, 28%) serum negative patients after liver transplantation. All the five patients developed viremia in the following three months.

Conclusions: Lux ™ primer-based real-time PCR is a sensitive test to quantitatively determine viral load in routine liver biopsy tissue. The test can be used for patients who have non-detectable serum HCV-RNA. The presence of HCV-RNA in the liver tissue can predict viral hepatitis recurrence. This test is potentially useful for monitoring patients after interferon combination therapy and liver transplantation.

1539 Diagnostic Value of D2-40, CD31 and CD34 in Detecting Angiolymphatic Invasion in Thyroid Follicular Carcinoma

YL Liu, X Lin, RS Saad, M Tung, JF Silverman. Allegheny General Hospital, Pittsburgh, PA.

Background: Separation of thyroid follicular carcinoma from adenoma relies on detection of vascular and/or capsular invasion. However, identification of angiolymphatic invasion can occasionally be challenging. We investigated which angiolymphatic markers can best evaluate angiolymphatic invasion in thyroid follicular carcinoma using immunohistochemical (IHC) vascular markers CD31 and CD34 and a specific lymphatic marker, D2-40.

Design: 30 thyroid follicular adenomas and 18 thyroid follicular carcinomas were retrieved from the hospital computer system. All follicular carcinoma was diagnosed when vascular and/or capsular invasion was histologically present. Immunostaining for D2-40, CD31 and CD34 was performed on an automated immunostainer with appropriate positive and negative controls. The cases positive for the IHC markers were counted and Chi-Square method was used for statistical analysis.

Results: 9 of 18 follicular thyroid carcinomas showed venous invasion, but not lymphatic invasion, with positive CD31 and CD34, and negative D2-40 staining. CD31 showed much less background staining than CD34.

Identification of angiolymphatic invasion of thyroid follicular carcinomas

Neoplasm	No.	D2-40	CD31	CD34
Carcinoma	18	0.0%	50.0%	50.0%
Adenoma	30	0.0%	0.0%	0.0%

Conclusions: 1. D2-40, a very sensitive and specific marker for lymphatics, is not useful in identifying vascular invasion in follicular carcinoma, since vascular invasion in follicular carcinoma involves venous channels, not lymphatics spaces.
2. CD31 is better than CD34 in identifying vascular invasion due to less background staining. We recommended using CD31 rather than CD34 and D2-40 in confirming vascular invasion in difficult cases.

1540 Does Smear Technique Affect the Accuracy of Intraoperative Sentinel Lymph Node Cytology in Breast Cancer?

NC Messias, ELC Alonsozana, GA Jockle, LS Logan, OB Ioffe. University of Maryland, Baltimore, MD; Mercy Medical Center, Baltimore, MD.

Background: Imprint cytologic examination is an accurate and fast method of intraoperative evaluation of sentinel lymph nodes in breast cancer. However, false-negativity rates have been reported to constitute up to 22%. Anecdotally, the scrape smear has been considered a better method to detect epithelial metastases than touch imprint. We studied whether the method of slide preparation and staining influences the accuracy of intraoperative sentinel lymph node cytology.

Design: Consecutive intraoperative smears of axillary sentinel lymph nodes examined from 1/2002 to 2/2004 were reviewed retrospectively. The smears from each lymph node consisted of a set of 4 slides: two touch imprints (TI), one stained with Diff-Quik (TI DQ) and the second with H&E (TI H&E); and two scrape smears (SC), stained in the same fashion (SC DQ, SC H&E). The smears were compared to the permanent H&E sections and cytokeratin immunostains. The histologic features of primary tumor and lymph node metastases were reviewed.

Results: 462 lymph nodes from 272 patients were included in the study. Of 383 smears interpreted as negative, 24 (6.3%) were positive on permanent sections, which showed macrometastases in 7, micrometastases in 15 and isolated tumor cells in 2 cases; and 11 (3%) were positive on cytokeratin immunostain, all as isolated tumor cells. On review, one TP DQ contained rare tumor cells (invasive lobular carcinoma, ILC). Of 14 smears deemed inconclusive intraoperatively, 5 (36%) were positive on permanent sections; on review 2 of those cases were positive, one on all 4 smears and one only on TP DQ. 65 cases were positive, all confirmed by permanent sections. The false-negative rate was 14.5% in ILC, and 4.4% in IDC, p=0.02; the inconclusive rate was 9.6% and 2% in ILC and IDC, respectively, p=0.01. TP DQ was false negative twice, TP H&E and SC H&E 4 times each, and SC DQ 6 times. 2 TP slides stained with DQ and H&E would have been as accurate as a complete set of 4 slides.

Conclusions: The most optimal combination of techniques for intraoperative axillary sentinel lymph node examination is 2 touch imprint preparations stained with DQ and H&E. Tumor type has a significant effect on the accuracy of intraoperative cytologic evaluation; therefore, prior knowledge of invasive lobular carcinoma diagnosis may be useful; in these cases, frozen section and/or ancillary intraoperative techniques such as rapid cytokeratin immunostain may prove useful.

1541 Enabling the Molecular Profiling of Clinical Specimens: A Novel Tissue Procurement Protocol for Translational Studies

WD Mojica, A Arshad, S Sharma, SP Brooks. SUNY @ Buffalo, Buffalo, NY.

Background: The goal of applying high throughput analysis (HTA) on clinical samples is hindered by several factors: tissue heterogeneity, degradation of nucleic acids and inaccessible protein epitoptes due to formalin cross-linking. Current tissue procurement protocols and the preparation of tissue for routine histological evaluation do not address or rectify these problems. Most attempts at devising recovery of cellular macromolecules use tissue that is either heterogeneous (snap frozen) or degraded/altered by formalin fixation. A novel, rapid tissue procurement protocol using manual exfoliation (ME) and immunomagnetic bead separation (IMBS) was developed and tested on clinical resection specimens. The goal was the isolation of sufficient quantities of homogeneous epithelial cells for HTA prior to routine processing. Since the procedure does not compromise the tissue, subsequent formalin fixation of the tissue can be performed and histological correlation with molecular results obtained.

Design: Surgical hemicolectomy specimens were obtained at the time of resection. Cells were manually exfoliated from selected areas (normal and tumor) and epithelial cells isolated using cytokeratin specific immunomagentic beads (Dynabeads Epithelial Enrich, Dynal Biotech ASA, Oslo, Norway) suspended in an RNA Later™ (Ambion)/ buffer solution. The enriched, homogeneous epithelial cells were disrupted and RNA, DNA and protein separated using Trizol™ (GIBCO BRL).

Results: ME + IMBS rapidly isolated purified, homogeneous epithelial cell populations (normal and tumor). Evaluation of RNA on an Agilent 2100 BioAnalyzer showed high 28S:18S rRNA ratios. Recovery of high molecular weight DNA was evident on electropheresis. Spectrophotometric analysis showed recovery of high quantities of nucleic acids. One dimensional analysis of proteins on an SDS/PAGE showed recovery of proteins with distinct quantitative differences between normal and tumor samples.

Conclusions: ME + IMBS is a simple, rapid, reproducible and cost effective technique for the isolation of a homogeneous epithelial cell population. The recovery of high quality, intact nucleic acids and proteins make this technique ideal for the preparation of clinical material for HTA. The technique does not destroy tissue architecture, thus allowing correlation between histology and molecular findings. The applicability of this technique to other tumor types is currently limited only by the specificity of the antibodies on the magnetic beads.

1542 Facilitating the Evaluation of Differential Protein Phosphorylation in Clinical Specimens: Combination of a Novel Tissue Procurement Protocol with a Fluorescent Phosphorylation Sensor Dye

WD Mojica, Y Piao, S Sharma, SP Brooks. SUNY @ Buffalo, Buffalo, NY.

Background: Phosphorylation of proteins represent the activation state of a cell. Analysis of phosphoproteins from clinical specimens is limited by the preparation of tissue. Snap frozen tissue contains a heterogeneous mixture of cells limiting its specificity. The use of antibodies on formalin fixed (FF) tissue requires the adequate and rapid fixation of tissue and often antigen retrieval techniques, resulting in variable sensititivty. A novel tissue procurement protocol involving manual exfoliation (ME) and immunomagnetic bead separation (IMBS) was used to improve the sensitivity and specificity of clinical tissue by isolating a fixative free, homogeneous epithelial cell population. This method, coupled with small molecule fluorophore detection technology (SMFDT), represents a simple, rapid and cost effective technique for the discovery of differentially phosphorylated proteins from clinical material.

Design: Separate groups of normal and tumor epithelial cells from colon resection specimens were isolated prior to fixation using ME followed by IMBS (Dynabeads Epithelial Enrich, Dynal Biotech ASA, Oslo, Norway). Cells were manually disrupted in a protective phosphate buffer (PhosphoSafe™, EMD). Equimolar concentrations of purified protein lysates were electropheresed on an SDS/PAGE followed by fixation and staining with a fluorescent dye (Pro-Q® Diamond Phosphoprotein Gel Stain, Molecular Probes). Phosphorylated proteins were documented on a Typhoon™ Variable Mode Imager (Amersham Biosciences) at wavelengths 530/580 nm for excitation/absorption.

Results: ME+IMBS resulted in separate purified, homogeneous populations of normal and tumor colonic epithelial cells. Sufficient quantities of protein were recovered for analysis. Phosphorylation status was maintained through cell lysis and protein purification. Quantitiative differences in protein phosphorylation was evident between the two electropheresed cell populations.

Conclusions: ME+IMBS is a technique capable of preparing a homogeneous epithelial cell population from clinical samples for proteomic analysis. The absence of FF and the use of SMFDT facilitates the sensitive detection of phosphorylated proteins. The matched cell populations exhibited differential protein phosphorylation. This simple, rapid, reproducible and cost effective protocol can be used to elucidate the phosphorylation status of proteins in specific cell populations from clinical material.

1543 Sensitive Method for *KRAS* Mutation Detection by Pyrosequencing™

S Ogino, T Kawasaki, M Brahmandam, L Yan, M Cantor, C Namgyal, E Giovannucci, M Mino, G Lauwers, M Loda, CS Fuchs. Brigham and Women's Hospital, Boston, MA; Dana-Farber Cancer Institute, Boston, MA; Harvard Medical School, Boston, MA; Biotage, Westborough, MA; Harvard School of Public Health, Boston, MA; Massachusetts General Hospital, Boston, MA.

Background: In tumors with mutant *KRAS* oncogene, typically there are a substantial amount of normal cells intermixed with tumor cells, in addition to wild type *KRAS* alleles that are often present in the tumor cells. Thus, *KRAS* mutation assay must be sensitive enough to detect a minority of mutant alleles among a large amount of wild type alleles.

Design: We developed Pyrosequencing™ (Biotage AB and Biosystems) method, a real-time, non-electrophoretic sequencing, for *KRAS* mutation detection, using three Pyrosequencing primers. Analytical sensitivity of this method was compared with conventional dideoxy sequencing by forward and reverse primers. Mixed DNA samples were prepared as follows; ratios of mutant cell line DNA (each one of 35G>T and 38G>A) to wild-type cell line DNA were 50:50, 30:70, 20:80, 10:90, 5:95, 3:97, and 2:98 (each with duplicated mixes); ratios of mutant DNA (each one of 35G>A, 35G>T, 34G>T, 34G>A, and 38G>A) from paraffin colon cancer tissue to DNA from normal paraffin tissue were 50:50, 30:70, 20:80, 10:90, and 5:95. We also compared *KRAS* sequencing results on 10 paraffin pancreatic cancer samples. Each DNA sample was tested in triplicate runs by each method. A number of runs with successful detection among a total number of runs were compared.

Results: Quantification of a mutant allele relative to a wild type allele by Pyrosequencing was linear in terms of various mixing ratios. In the cell line DNA mixing study, Pyrosequencing detected in significantly more runs for the 10:90, 5:95, 3:97, and 2:98 mixes (24 of 24 runs even for the 2:98 mix) than dideoxy sequencing ($p < 0.01$, $p < 0.001$, $p < 0.005$, and $p < 0.001$, respectively). In the paraffin DNA mixing study, Pyrosequencing detected in significantly more runs for the 20:80 and 10:90 mixes (15 of 15 runs even for the 10:90 mix) than dideoxy sequencing ($p < 0.01$ and $p < 0.005$, respectively). For 7 pancreatic tumors with *KRAS* mutations, Pyrosequencing detected in 20 of 21 runs, whereas dideoxy sequencing detected in 12 of 21 runs ($p < 0.05$).

Conclusions: Our Pyrosequencing method is very sensitive for the detection of a small amount of mutant *KRAS* alleles in a background of a large amount of wild-type alleles, and useful for tumors containing a large amount of normal cells.

1544 Computerized Diagnostic Consultation System for Hepatobiliary Pathology

DA Ostler, S Ninan, Z Qu. UT-MS Houston, Houston, TX.

Background: The exponential growth of medical knowledge has resulted in an enormous amount of new diagnostic information. The limited knowledge base of an individual relative to the large amount of complex diagnostic information can often be a source of diagnostic errors, especially in specialized fields. Hepatobiliary pathology as a subspecialty deals with a wide spectrum of disease entities now often encountered by general pathologists due to increasing popularity of liver needle core biopsy. The

overlapping morphological features and clinical presentations of many liver diseases make the diagnosis a new challenge to many general pathologists. As part of a continuous endeavor to build an expert system for surgical pathology[1], a consultation system is constructed to aid in the diagnosis of common liver diseases.
Design: Clinical features, histologic features and relevant laboratory findings of approximately 280 liver diseases/variants are integrated into a relational database (Microsoft Access). More than 80 morphologic features are included to describe the diseases and thus are used as search keywords. Common synonymous terms are collected and a string manipulation of computer query language (asp.net) is designed to circumvent natural language pluralism[1]. The system is implemented and accessible on the World Wide Web at http://dpalm.uth.tmc.edu/faculty/bios/qu/qudemo/dropdownace.aspx
Results: The system allows retrieval of diagnosis by any one or combination of relevant attributes such as mode of inheritance, disease nature etc. When a user provides observed clinical and morphological findings of an unknown case, the system can generate a list of differential diagnoses by pattern recognition. It recognizes different forms of synonymous terms and has relaxed restriction in search phrases. With salient diagnostic information of these diseases, it also directs the user's attention to specific diagnostic features, to help select additional studies and make well-informed diagnostic judgments.
Conclusions: This system differs from books-on CD or web-based information systems in that it provides practical diagnostic consultation by generating differential diagnoses for unknown cases. The thesaurus search significantly improves its practical application. It not only helps make detailed diagnostic information in hepatobiliary pathology manageable to many general pathologists, but also serves as a model for information management in surgical pathology.
1.Kuruvilla S et al: A computer-assisted Diagnostic System for Surgical Pathology. ASCP/CAP annual meeting 2002.

1545 Application of Chromogenic In Situ Hybridization (CISH) in the Differential Diagnosis of Renal Tumors

MA Palau, R Ronchetti, WM Linehan, EM Li Ning, C Torres-Cabala, MJ Merino. National Cancer Institute, Bethesda, MD.
Background: One of the characteristics of renal cell tumors is their morphologic heterogeneity which is reflected at the genetic level. Papillary configuration is common to most types of renal neoplasms but it is the predominant pattern found in type 1 and type 2 tumors. Genetically, PRCC type 1 is identified by trisomies or tetrasomies in chromosomes 7 and 17 and the loss of chromosome Y. The genetic changes associated with type 2 are not well known. In this study we performed CISH to investigate numeric alterations in chromosomes 7 and 17 in a wide spectrum of renal tumors to determine the role of CISH as a helpful tool for the surgical pathologist in the diagnosis of these tumors.
Design: Ninety renal cell tumors, 28 type 1 PRCC (8 sporadic, 9 hereditary and 11 unknown) and 62 cases representing the spectrum of renal tumors (18 clear cell RCC, 10 oncocytomas, 9 type 2 PRCC, 8 chromophobe, 4 medullary, 6 CDC, 2 metanephric adenomas, 4 hybrid tumors, and 2 unclassified) were studied. All cases were classified following the WHO classification. CISH was performed utilizing commercial probes for chromosomes 7 and 17. Cases were categorized as diploid (two copies) or aneuploid if they had three or more copies in more than 10% of tumor cells.
Results: Fifteen type 1 PRCC tumors showed aneuploidy for chromosome 7 (9 hereditary, 3 sporadics and 3 unknown) and 13 cases were diploid. Seven cases were aneuploid for chromosome 17 (5 hereditary and 2 unknown). Three type 2 PRCC were aneuploid for chromosome 7 and 2 for chromosome 17. Aneuploidy for chromosome 7 was also found in 3 clear cell RCC, one CDC, one chromophobe, and 1 unclassified tumor. Aneuploidy for chromosome 17 was detected in 2 chromophobes and one unclassified.
Conclusions: These results indicate that CISH is a useful tool for pathologists to identify chromosomal abnormalities and to improve the diagnosis of renal tumors. There is a clear correlation between aneuploidy for chromosome 7 identified by CISH and hereditary PRCC type 1. Absence of aneuploidy for chromosome 17 can help to identify sporadic PRCC type 1. Identification of aneuploid RCC clear cells with sarcomatoid features for chromosome 7 suggests high grade and new hits in tumor progression.

RESULTS

Histology	Cases	Ch 7 Aneuploidy	Ch 7 Diploidy	Ch 17 Aneuploidy	Ch 17 Diploidy
TYPE 1 PRCC	28	15	13	7	21
Hereditary	9	9	0	5	4
Sporadic	8	3	5	0	8
Unknown	11	3	8	2	9
TYPE 2 PRCC	9	3	6	2	7
OTHERS	53	6	47	3	50

1546 "Amyloid Chip" for Tissue Detection and Characterization of Deposits by SELDI-MS Spectrometry

MM Picken, V Thulasiraman, RN Picken, L Lomas. Loyola University Medical Center, Maywood, IL; Hines VA Hospital, Hines, IL; Ciphergen Biosystems Inc, Fremont, CA.
Background: The gold standard of amyloid diagnosis is detection of deposits in tissues, either by Congo red or by electron microscopy. This detection is subject to low sensitivity, and the typing of deposits by immunohistochemical methods is frequently unreliable. We have explored the applicability of proteomic technology to amyloid detection and typing.
Design: Surface enhanced laser desorption/ionization-Mass Spectrometry (SELDI-MS) is a technology that combines solid-phase extraction chromatography with direct detection by mass spectrometry. SELDI-MS surfaces were derivatized to generate uniquely selective ProteinChip® Arrays designed to detect specific properties of amyloid deposits.
Results: Tissue was mechanically disrupted in lysis buffer, spun and the supernatant was aliquoted and frozen at –80°C. At the time of analysis, supernatant was incubated with bead affinity reagent and washed. Bound proteins were extracted with 50% acetonitrile + 0.3% TFA, and re-concentrated on a ProteinChip® Array. After a final wash, 1ul of sinapinic acid was applied and the array analyzed using a mass reader (model PBSIIc; Ciphergen). We tested myocardium, kidney (cortex and medulla) spleen and urinary bladder. Positive samples included amyloid derived from transthyretin (ATTR), immunoglobulin lambda light chain (AL) and AA; for controls, amyloid negative samples were used. Only the known positive samples showed distinct peak(s) with molecular weight(s) corresponding to the monomer of TTR, AA protein or the light chain fragments.Preliminary results indicate that such surfaces are able to capture clusters of proteins of the expected masses of amyloid proteins. These clusters were not seen in corresponding negative control tissues. When comparing these protein clusters between different tissues, unique profiles were detected. Further characterization of these captured proteins is necessary to confirm their disease process specificity
Conclusions: ProteinChip® Arrays derivatized with affinity ligands specific for amyloid deposits may represent a unique opportunity to develop a simple and rapid test for amyloid detection in tissues. Our preliminary studies indicate that this technology can be used to detect and analyse at least three of the most frequent types of amyloid in unfixed tissue samples. Further studies are needed to assess whether this protocol offers a higher sensitivity for the detection of amyloid deposits than currently used methods.

1547 Cell Clots: An Efficient and Accurate Method of Converting Cell Suspensions into Blocks for Immunohistochemical Staining

A Polydorides, E Hyjek, A Chadburn. Weill Cornell Medical College, New York, NY.
Background: Immunophenotyping of fluid specimens relies on flow cytometry (FC) and immunohistochemical staining (IHC) of smears, thin preps and cell blocks (CB). These approaches are compromised by the need to adapt FC to detect intracellular antigens, contaminating non-lesional cells, debris and endogenous enzymes in smears, lack of malignant cells in some thin preps and disintegration of CB pellets in processing. We describe a method of generating CBs in a thrombin-fibrin matrix (cell clot; CC) that largely circumvents these problems and provides IHC results similar to tissue section IHC or FC.
Design: CCs were generated from cell suspensions of 25 peripheral bloods (PB), 24 bone marrow aspirates, 3 lymph nodes and 2 pleural fluids from 33 CLL, 16 acute leukemia (AL) and 3 mantle cell lymphoma (MCL) pts. The cells were pelleted in eppendorf tubes (cell number per sample 5-50 million), resuspended in 30-50µl of fibrinogen (5mg/ml) to which 5U of thrombin was added, mixed, left for 2-3 min to clot and briefly spun down. Formalin was added and the CCs were routinely processed. Normal PB fixed in formalin, B5 or Bouin's was similarly prepared. Paraffin tissue sections from each CC were cut for routine staining or CD3, PAX5, ZAP70, BCL1 and/or TdT IHC using antigen retrieval and detection systems applied to tissue sections. Results of CC IHC were compared with FC and/or tissue IHC. Results within 10% were considered concordant for CD3 and PAX5; ZAP70, BCL1 and TdT were evaluated as positive (pos) or negative (neg) with ZAP70 considered pos if >20% CD3.
Results: CC sections were seen on all stained slides; H&E stained CC sections had no significant artifacts. CC IHC for CD3 (32 cases) and PAX5 (15 cases) showed 93% concordance with CD3 and CD19 expression by FC. IHC for ZAP70 in 32 CLLs was concordant with FC or tissue IHC in 20 (63%) cases; all discordant cases were CC IHC pos, decalcified tissue IHC and/or FC neg. The 14 TdT pos and 2 TdT neg ALs by FC and tissue IHC were similarly pos or neg by CC IHC; in 87% the number of pos cells was similar. All 3 MCLs were BCL1 pos by CC and tissue IHC. Immunostaining of formalin, B5 and Bouin's fixed CCs for CD3, PAX5 and ZAP70 gave similar results except for less nuclear staining for ZAP70 with B5 fixation. CC IHC showed little background staining, including of the thrombin-fibrin matrix.
Conclusions: Cell clots generated within a thrombin-fibrin matrix allow for efficient and accurate immunostaining and decreased specimen loss in processing and staining.

1548 Multiplex STR and Mitochondrial DNA Testing for Paraffin Embedded Specimen of Healthy and Malignant Tissue: Interpreation Issues

DA Popiolek, P Illei, BA West, M Prinz, ZM Budimlija. New York University School of Medicine, New York, NY; NYC Office of Chief Medical Examiner, New York, NY.
Background: DNA-based polymerase chain reaction coupled with microdissection is a powerful tool for confirming the presence of suspected contaminant tissue/cells in surgical pathology or cytology material. Short tandem repeat (STR) analysis of tumor DNA can show allelic instability or mitochondrial DNA (mtDNA) sequence variation. The aim of this study was to determine whether this variability influences the validity of STR analysis of tumor DNA for determining sample identity.
Design: A total of 55 pairs of non-neoplastic vs. malignant tissues from the same individuals were tested using the PowerPlex®16 multiplex STR kit, which simultaneously tests 15 STR loci and the Amel locus o X/Y chromosome (Promega), and the Linear Array mtDNA HVI/HVII Region Sequence Typing kit, an assay based on sequence specific oligonucleotide (SSO) probe analysis of hypervariable mtDNA d-loop regions I and II (Roche Molecular Systems).

Results: The analysis of 10 different groups of malignant tumors (endometrial adenocarcinoma – types I and II, granulosa cell tumor, adenosarcoma, malignant mixed Mullerian tumor, adenocarcinomas of prostate, lung, colon and cecum and cutaneous melanomas) were performed. Complete/partial DNA profiles were determined for all samples. Most STR allele profiles showed degradation effects (imbalance and allelic drop out). Much better success was notable for loci of low molecular weight DNA, again consistent with DNA degradation. Nevertheless several sample pairs showed results consistent with loss of heterozygosity (LOH) or microsatellite instability. The allele designation of the tested hypervariable mtDNA d-loop regions I and II refer to particular polymorphisms present within each region. Differenceswithin the experimental tissue pairs in this study were observed in several cases, implying possible mtDNA heteroplasmy and/or cross contamination due to the high sensitivity of mtDNA assay.

Conclusions: The use of the described identity testing systems is a valuable method for determining the origin of malignant tissue, despie tumor DNA instability. Distinction of DNA degradation effects from true LOH can be challenging at times. Thus interpretation guidelines should incorporate signal intensity and molecular weight of affected alleles. For mtDNA testing mutation and heteroplasmy issues will be difficult to establish unless histology specimen can be processed under ultra clean conditions.

1549 Tissue Array Construction: Pitfalls, Problems and Progress

A Quinn, P Tang, Q Yang, P Bourne. University of Rochester Medical Center, Rochester, NY.

Background: The tissue array has become a popular tool for high throughput analysis of fixed tissues because it maximizes tissue conservation and economizes research. This study sought to find the best conditions by which to manipulate fatty and fibrous tissue. As a corollary, to ensure that a feature dotted on a slide is accurately removed from its block, fatty and fibrous tissue sections were cut and analyzed for distortion.

Design: 3 blocks each from 2 breast cases were built into 3 arrays, each comprised of cores of different diameters. Two additional variables, the tissue nature (fatty, fibrous or mixed) and the 4°C incubation period of the tissue, were structured into the grid of each array. Core transfer rates (CTRs) were calculated for each variable. In addition, 3 blocks each from 2 breast cases were cut into 6 µm-thick sections, then transferred to waterbaths at temperatures of 34, 38, 42, 46 and 50°C, and mounted on slides. The cut sections were routinely stained and analyzed for distortion relative to their blocks.

Results:

Core Transfer Rates

Core Diameter (mm)	Room Temperature	3 Hours at 4°C	24 Hours at 4°C
0.6	93.3%	100.0%	100.0%
1.0	73.3%	80.0%	90.0%
1.5	40.0%	86.7%	83.3%

CTRs were highest when punches were made with 0.6 mm diameter cores from blocks that had been stored at 4°C for either 3 or 24 hours. No tissue type showed a particular affinity for being punched, though the fibrous tissue was the most resistant. An exact temperature for minimal section distortion was difficult to quantify due to internal type variations. However, waterbath temperatures above 42°C resulted in more distortion, particularly with fibrous tissue. Overall, tissue sections tended toward a left-right expansion and a top-bottom compaction, suggesting a crushing effect by the microtome blade.

Conclusions: Tissue is best conserved if arrays are made with smaller cores from tissues that have been stored at 4°C for at least 24 hours. CTRs could be higher if pathologists and technicians avoid features with fibrous inclusions. CTRs also suffer as core diameter increases, a tendency that limits the block-preservation efficacy of tissue arrays. Tissue section distortions are subject to not only high waterbath temperatures, but to the crushing effect of microtome blades as well, ultimately undermining tissue array projects by hindering core removal accuracy. Though these results are applicable to other tissue array models, further studies are needed to determine which conditions best suit a given tissue.

1550 A Virtual Microscopy Image Database for Liver Pathology Education

C Reading, L Proctor, Y Shen, J Woosley. University of North Carolina, Chapel Hill, NC.

Background: A comprehensive collection of high quality histologic slides is essential for education of pathology trainees in liver pathology. However, maintenance of the quality of the teaching slide collection is constantly challenged by slide loss, breakage, and stain fading. Recut replacement slides are not always easily attainable, considering the small size of most liver core biopsies. When recuts can be obtained, the most important diagnostic features may not be well represented.

Design: The ScanScope (Aperio Technologies) virtual microscopy instrument and software have been used to create a liver pathology image database. This instrument is an ultra-fast, linear-array based slide scanner. Histologic sections on glass microscope slides are scanned to obtain a high-resolution digital image of the entire section (virtual slides). Slides are scanned using a X20 objective. This magnification is optimal for demonstrating most pathologic processes, where low or intermediate power pattern recognition is of primary diagnostic importance. At this scanning magnification, there are some minor limitations in clarity of fine nuclear detail in virtual slides, but this is rarely a critical shortcoming. Most sections can be scanned in less than 5 minutes. Image files are compressed using JPEG2000 wavelet technology, creating image files of manageable size without compression artifacts. The image compression software permits some degree of control over specimen orientation, color balance, and contrast, although the sophistication of image manipulation is considerably less than that attainable with conventional digital imaging software (i.e. Adobe Photoshop). When more control over image editing is required, the ScanScope image files can be re-compressed and can be opened in Photoshop and manipulated like any digital image.

Results: A pathology educational database of over 100 virtual liver biopsy slides has been created.

Conclusions: Images can be viewed with the ImageScope virtual slide viewing software (available as a free download from Aperio Technologies). The software is intuitive to use and closely mimics viewing of a slide at the microscope. In addition, image annotations can be added to enhance the learning experience. Virtual slide image quality is nearly equivalent to that seen at the microscope. Unique teaching slides can be reproduced in unlimited quantities and slides are never lost, broken, or misfiled. Internet, intranet, or DVD access permits continuous availability of a teaching slide collection to trainees.

1551 Step Sectioning Increases Diagnostic Yield of Melanoma Micrometastases in Sentinel Lymph Nodes with MCW Melanoma Cocktail

VB Shidham, R Komorowski, P Gupta, L Parameswaran, CC Chang, W Dzwierzynski. Medical College of Wisconsin, Milwaukee, WI; The Methodist Hospital, Houston, TX.

Background: The likelihood of detecting melanoma positive sentinel lymph nodes (SLNs) increases with step sectioning. But, the dilemma is how many step sections to evaluate! Plurality of step sections with multiple antibodies further increases the cost and complexity of evaluation. The 'MCW melanoma cocktail' offers many benefits including ease of interpretation.

Design: We studied SLNs from 42 clinical stage I/II melanoma cases (Table 1). Three levels (#2, 5, & 8) of formalin-fixed paraffin-embedded tissue sections of SLNs at interval of 200 µ were examined with HE. The levels adjacent to each of these HE sections (#1, 4, & 7) were evaluated for melanoma metastases utilizing the MCW melanoma cocktail by previously published protocol (Shidham et al, BMC Cancer 2003,7;3(1):15 http://www.biomedcentral.com/qc/1471-2407/3/15). Levels #3, 6, & 9 were processed as negative controls.

Results: The increase in the number of positive cases from 10.6 with 1 level to 16 with 3 levels (Table 1) was statistically significant (proportion test, $p < .05$). This further increased to 13 with 2 levels; however, the difference was statistically insignificant. Benign capsular melanocytic nevi were observed in 4.3 cases with 1 level, in 4.6 cases with 2 levels, and in 7 cases with 3 levels (1 case had concurrent melanoma metastases).

Conclusions: Three step levels of SLNs at 200 µ intervals immunostained with the 'MCW melanoma cocktail' detected a higher number of cases with melanoma metastases. With 2 levels, the increment in the number of positive cases, although consistent, was statistically insignificant. Routine evaluation of more than 3 levels may be less productive and impractical. The use of the cocktail for 3 levels would significantly reduce the cost and the pathologists' time/effort when compared to 9 slides (3 individual immunomarkers x 3 levels) if component immunomarkers have to be used individually. The number of benign capsular melanocytic nevi also increased with the number of levels evaluated.

Melanoma metastases in SLNs.

			Positive for Melanoma metastases		
Levels		Slices (n=405)	Blocks (n=116)	SLN (n=83)	Cases (n=42)
One level	1 alone	50	17	11	10
	4 alone	36	15	11	10
	7 alone	40	19	14	12
	Mean	42	17	12	10.6
Two levels	1+4	51	18	12	11
	1+7	52	21	16	15
	4+7	42	20	15	13
	Mean	48.3	19.6	14.3	13
Three levels	1+4+7	80	30	22	16

1552 The Diagnostic Utility of Immunostaining for Angiotensin Converting Enzyme (CD143) and CD4 in the Workup of Granulomatous Inflammation

HK Singh, K Wilson, JW Woosley, SV Seshan, E Hjyek, V Nickeleit. The University of North Carolina, Chapel Hill, NC; East Carolina University, Greenville, NC; New York Presbyterian Hospital/Cornell Medical College, New York, NY.

Background: The differential diagnosis of granulomatous inflammation is broad and the major differential diagnostic considerations are sarcoidosis, infectious diseases, and drug reactions, each requiring different treatment modalities. The exact differential diagnosis based on light microscopical features can be very difficult. Immunohistochemical staining may prove to be a useful adjunct diagnostic tool to render a specific diagnosis. However, the immunohistochemical staining profile of granulomatous inflammation has hitherto not been defined.

Design: Immunohistochemical stains for monoclonal antibodies against ACE (CD143), CD68, CD3, CD4, CD8, CD20, and CD138 were performed on formalin fixed tissues from 46 cases of sarcoidosis (19 kidney, 17 skin, and 10 lung). Controls: 5 confirmed cases of drug induced granulomatous interstitial nephritis, 5 cases each of confirmed mycobacterial and fungal granulomas, and 3 cases of granulomatous granuloma annulare(GA). Scoring of staining (semi-quantitative): 1)(ACE, CD68, CD3, CD4, CD8, CD20, CD138): % cell positive in granulomas, % multinucleated giant cells, and % inflammatory infiltrates. 2) additional for ACE: intensity of cellular staining (0-3+); presence or absence of ACE+ histiocyte cell clusters (≥3 cells in intersititum away from granulomas). Statistical analysis was performed using ANOVA and discriminate analysis.

Results: Statistically significant differences ($p<0.001$) were seen for ACE and CD4 staining. Only cases of sarcoidosis and mycobacterial granulomas showed strong staining for ACE in >50% of cells in granulomas, multinucleated giant cells, and histiocytic cell clusters. Negative or only focal weak ACE staining was seen in fungal and drug induced granulomas, and GA. Intra-granulomatous CD4 staining was significantly increased in mycobacterial vs. sarcoid granulomas, fungal vs. drug induced granulomas, and sarcoidosis vs. GA.

Conclusions: Immunohistochemical staining for ACE and CD4 can be used to discriminate between granulomas caused by sarcoidosis, drug reactions, mycobacterial and fungal infections, and GA.

1553 A Simple One-Tube Method for DNA Isolation and Polymerase Chain Amplification of Fresh and Paraffin-Embedded Tissues

LR Sorbara, S Dieffenbach, T Pham, TH Pham, M Raffeld. National Institutes of Health/NCI, Bethesda, MD.

Background: Hematopoetic malignancies are difficult to diagnose without the supportive data of immunohistochemical, flow cytometric, and molecular analyses. The polymerase chain reaction (PCR) method of amplification has become routine in the analyses of both fresh and formalin-fixed, paraffin-embedded tissue samples. Although PCR technology has simplified molecular studies, issues regarding limited tissue availability and loss of template resulting from multi-step DNA purification procedures, remain problematic.

Design: In this study, we report the use of a commercially available resin, *Gene Releaser* (Bioventures, Inc.) for the one-tube, one-step purification and PCR amplification of formalin-fixed, paraffin-embedded tissue samples in routine diagnostics. Approximately 500 samples submitted to the clinical service were prepared by traditional enzymatic digestion and extraction prior to analyses. The amplification ability of these traditionally prepared samples was compared to more than 1000 routine samples prepared with *Gene Releaser*.

Results: Results showed that the overall percentage of cases that could be amplified increased from 88% with traditional methods to 96.8% with the *Gene Releaser* method ($p = 0.0001$).

Conclusions: This improvement may be attributed to both the decreased loss of tissue during the DNA preparation, and the sequestration of inhibitory factors by *Gene Releaser*. *Gene Releaser* has also reduced the turnaround time of reporting results by several days when compared to traditional methods.

1554 Expression Profiling of Microdissected Endothelial Cells from Colorectal Cancer

M Sridhar, AM Jubb, LA Strickland, Z Modrusan, WL Ince, TD Wu, H Koeppen. Genentech Inc, South San Francisco, CA.

Background: Tumor-associated endothelial cells have an expression profile that is distinct from endothelium associated with normal tissue. This differential expression is not readily apparent from microarray experiments conducted on tissue homogenates, due to the small percentage of endothelial cells in the tissue. Microdissection of normal and malignant colon tissue may be used to enrich for endothelial cells and could potentially yield new cancer-specific targets for anti-angiogenic therapy.

Design: Normal and malignant frozen colorectal tissues were obtained from the Genentech archive. Endothelial cells were immunofluorescently labeled with a CD146 antibody conjugated to Alexafluor-546 and microdissected using the MMI SL-microCUT. RNA was extracted using the Arcturus RNA picopure kit and RNA quality was measured with the Agilent bioanalyzer. Amplification was performed with Agilent's low input fluorescent amplification kit. Representivity of the amplified RNA was confirmed using quantitative reverse-transcriptase PCR for genes of low and high abundance. Cy5-labeled, amplified RNA was hybridized to the Agilent whole genome microarrays and microarray data was analyzed with Rosetta Resolver v4.0. Enrichment for endothelial cells was validated in the datasets using known endothelial markers. Contamination of the samples was assessed using known markers for epithelial, smooth muscle and inflammatory cells.

Results: Endothelial-specific datasets were compared with microarray data from whole tissue and dissected epithelium to distinguish endothelial-specific genes. Potential anti-angiogenic targets were identified from those showing strong expression in cancer endothelium and weak expression in normal endothelium. Several genes showed increased expression in tumor-associated vasculature compared with normal-associated vasculature, including novel transcripts and molecules previously reported in the literature. A complete gene list is being assembled and will be presented at the meeting.

Conclusions: Microdissection is a powerful tool for the enrichment of endothelial cells and may yield valid targets for anti-angiogenic therapy. Studies are ongoing to validate the microarray dataset using *in situ* techniques, which permit the assessment of endothelial expression.

1555 Use of Array-Based Comparative Genome Hybridization To Distinguish Hepatic Adenoma from Hepatocellular Carcinoma

BA Stohr, LD Ferrell, FM Waldman, K Mehta, S Kakar. UCSF Medical Center, San Francisco, CA.

Background: Hepatic adenomas (HA) can be difficult to distinguish from well-differentiated hepatocellular carcinomas (HCC) on morphologic criteria alone. This distinction is particularly difficult when well-differentiated hepatic neoplasms occur in atypical demographic settings like males or patients above 60 years of age. Establishing the correct diagnosis in these cases is critical in guiding management decisions. Comparative genome hybridization (CGH) has demonstrated that genomic instability is not observed in typical HA, while a consistent pattern of chromosomal gains (*e.g.* 1q, 7q, and 8q) and losses (*e.g.* 16q) is observed in HCC including well-differentiated ones. However, the role of CGH in the evaluation of well-differentiated 'adenoma-like' tumors is not clear.

Design: Array-based comparative genomic hybridization was performed on two well-differentiated hepatic neoplasms occurring sequentially in a 65-year old male. The patient underwent wedge resection for a 5 cm liver mass. Serum AFP was normal and there was no evidence of chronic liver disease. The tumor showed 1-2 cell thick liver plates, lack of cytologic atypia, and preservation of reticulin architecture. Thus, the tumor had all of the histologic features of a typical HA, but its occurrence in an elderly male was unusual. Two years later, the patient presented with a 3 cm liver tumor which demonstrated widened cell plates, mild cytologic atypia, and focal loss of reticulin framework. These features met the criteria for the diagnosis of well-differentiated HCC. Array-based CGH was performed on both the original 'adenoma-like' tumor and the subsequent HCC.

Results: Gains of chromosomes 1q, 4q, 7q, and 8q were observed in both the original 'adenoma-like' tumor and the subsequent HCC, with the latter tumor also demonstrating gains of chromosomes 9, 16, 17, 20, and X. Because gains at chromosomal loci 1q, 7q, and 8q are typical of HCC and are not observed in HA, these results suggest that the initial 'adenoma-like' tumor is in fact best characterized as a well-differentiated HCC, with the subsequent tumor representing a recurrence with additional chromosomal abnormalities.

Conclusions: Well-differentiated hepatic neoplasms resembling hepatic adenomas in elderly males may represent well-differentiated hepatocellular carcinoma. Array-based CGH analysis can be useful in the differential diagnosis of well-differentiated hepatic neoplasms.

1556 Enzyme Metallography (EnzMet) — A Robust Detection System for High Resolution Ultrasensitive Immunohistochemistry (IHC)

RR Tubbs, J Pettay, PC Roche, W Powell, RD Powell, T Grogan, JF Hainfeld. Cleveland Clinic Foundation, Cleveland, OH; Ventana Medical Systems, Inc., Tucson, AZ; Nanoprobes, Inc., Yaphank, NY.

Background: Alternatives to conventional immunohistochemistry (IHC) have been sought to improve sensitivity and resolution, and to minimize diffusion associated with conventional IHC.

Design: Multi-tumor tissue microarrays TMA) containing a total of 86 tumor cores from multiple lung, head and neck, renal cell, colorectal, and urothelial carcinomas were evaluated by automated enzyme metallography (EnzMet)™ (Nanoprobes) using EGFR and Ki-67 as model systems for localization of cytoplasmic membrane and nuclear antigens respectively. Sites of antigen localization were visualized via deposition of metallic silver through the EnzMet procedure. EnzMet was accomplished using fully automated on-line cell conditioning via the Benchmark™ immunostainer, commercially available primary antibodies, and I view SA-HRP (Ventana). Slides were scored by conventional light microscopy and compared to results using conventional automated DAB immunoperoxidase staining.

Results: There was excellent corzrelation between the results obtained with conventional immunohistochemistry for cytoplasmic membrane (EGFR) and nuclear (Ki-67) immunostains. In addition, very sharp high resolution localization was achieved with enzyme metallography with no diffusion outside the area of localization.

Conclusions: Enzyme metallography represents an excellent brightfield immunophenotypic alternative to conventional immunoperoxidase techniques, facilitating high-resolution morphologic analysis of subcellular compartments in human tumors.

Supported by NIH SBIR grants 1R43 GM64257-01 and 5R42 CA83618-03

1557 An Approach to High Throughput Automated Multi-Color FISH Scanning of Tissue Microarrays

RR Tubbs, E Swain, J Pettay, M Hartke, K Keslar, K Simmerman, MP Bronner, D Hicks, J Crowe, M Skacel. Cleveland Clinic Foundation, Cleveland, OH.

Background: Tissue microarrays are valuable tools for morphologic validation of array-based comparative genomic hybridization (ACGH) and other translational research applications requiring independent verification of genomic gains and losses by fluorescence in situ hybridization (FISH). However, maintaining proper spatial orientation and accurate tracking of the multiple arrays of tissue cores on individual slides during manual scoring is challenging and prone to error.

Design: We used consecutive sections of a moderately complex tissue microarray consisting of 14 tissue cores (12 invasive breast carcinomas, a liver core for spatial orientation, and an on slide positive control core) to evaluate the performance of TMA tracking software (MAT) applied to captured image files from a high throughput FISH scanner (MetaSystems). FISH results from three molecular pathology technologists experienced in FISH counting (36 cores) were compared to the results of 220 successfully captured cores in a series of twenty-six, 12 core TMAs analyzed by the FISH scanner and the MAT tracking software. Computerized automated classifiers for CEP17/*HER2*/*TOP2A* FISH signals and their derived ratios were applied to the TMAs.

Results: There was excellent overall agreement between the manual and automated locus enumeration results and calculated ratios. There was agreement as to the presence or absence of *HER*2 gene amplification in 94% of the 12 cores as assessed by both manual and instrument methods. Genotype heterogeneity in two of the cores accounted for most of the discordances. Consecutive sections of the cores in the TMAs did demonstrate minor variability, comparable to the precision associated with manual counting.

Conclusions: High throughput large-scale tissue microarray validation via FISH for documenting genomic gains and losses identified by ACGH and other extraction based assays appears feasible using an automated scanner and tracking/classifying software. This automated approach markedly facilitates target verification in genomic research.

1558 Tissue Microarrays with Paraffin Tissue Core Biopsies of 0.43 mm in Diameter Are Technically Feasible

UF Vogel, BD Bueltmann. University Clinic Eberhard-Karls-University, Tuebingen, Baden-Wuerttemberg, Germany.

Background: As introduced by Kononen et al. in 1998, tissue microarrays (TMAs) are paraffin blocks containing up to 1000 cylindrical paraffin tissue core biopsies (PTCBs). TMAs are especially suited for screening large amounts of tumor samples for those genes which are expressed by most of the tumor cells within a certain sample. The TMAs are intended to harbour as much PTCBs as possible to maximize the benefits of the TMA technique. Till now, the minimal diameter of the PTCBs is 0.6 mm. Smaller diameters were said to be impossible due to the breakage of the tissue punch. To increase the number of PTCBs per TMA, we tried to construct TMAs with PTCBs of 0.43 mm in diameter.

Design: Routinely used hypodermic needles (22G, inner diameter: 0.43 mm; outer diameter: 0.7 mm; Sterican, B.Braun Melsungen AG, Germany) were shortened to a length of about two centimeters and resharpened by a drill grinder with a cutting disc (Professional Grinder IB/E, Proxxon, Germany). For pushing the punched PTCBs out of the needles stylets were constructed also out of hypodermic needles whose outer diameter corresponded to the inner diameter of the needle-made punches (27G; outer diameter: 0.40 mm, Sterican, B. Braun Melsungen AG, Germany). The holes in the recipient paraffin blocks were drilled using a drill of 0.43 mm in diameter (Hartner GmbH, Germany). The PTCBs were punched out of paraffin tissue blocks and manually transferred to the predrilled recipient blocks. According to routine methods, the filled TMAs were cut and the sections stained.

Results: The construction of tissue punches and stylets out of routinely used hypodermic needles was simple and cheap. The tips of these punches of 0.43 mm in inner diameter were strong enough to obtain PTCBs from donor paraffin tissue blocks without breakage. The manual transfer of the PTCBs to the predrilled holes of the TMAs was easy when using an illuminated magnifying glass. The cutting of the TMAs and the staining of the sections was comparable to those TMAs with larger PTCBs. The small 0.43 mm diameter of the PTCBs was sufficient to get enough cells for evaluation.

Conclusions: Tissue microarrays with PTCBs of 0.43 mm in diameter are technically feasible. This small diameter is sufficient to obtain enough cells for the evaluation of gene expression and gene copy number.

1559 Fluorescence In Situ Hybridization of Already Stained Paraffin Sections Mounted on Uncoated Slides - What To Do?

UF Vogel, BD Bueltmann. University Clinic, Eberhard-Karls-University, Tuebingen, Baden-Wuerttemberg, Germany.

Background: Especially concerning small biopsies, the whole paraffinized material may be consumed for step sectioning and routine stainings. Therefore, no material is left for additional stainings like fluorescence in situ hybridization (FISH). Under these circumstances, FISH may be performed on the already routinely stained sections. However, because of the use of uncoated slides in routine laboratories, these sections will float off the slide during the pretreatment procedures for FISH. Therefore, we looked for techniques to overcome this problem.

Design: Already routinely hematoxylin-eosin stained and coverslipped sections were placed in xylene to remove the mounting medium (pertex, medite, Germany) and the glass coverslip. Then three different methods were used:

1.The stained sections were scraped off the slide with a trimming knife (trimming knife handle F-80, Feather Safety Razor CO., LTD, Japan), reembedded in paraffin, cut and mounted on coated slides (SuperFrostPlus, Langenbrinck, Germany).

2.The stained sections were covered with a thin layer of liquid hot paraffin and then lifted off the slide by using the trimming knife with a new, sharp microtome blade. This sandwich of paraffin and tissue was transferred to a warm water bath (42 C) and then mounted on a coated slide (SuperFrostPlus, Langenbrinck, Germany).

3.A sticky, so-called tape window was put on the stained sections. Then the sections were lifted off the slide by using the trimming knife with a new, sharp microtome blade and transferred to a specially coated slide using the paraffin tape transfer system (Instrumedics, Hackensack, NJ, USA).

By using these techniques, finally, the sections were mounted on coated slides and were further processed using routine FISH pretreatment protocols and DNA-directed probes.

Results: With all three techniques, FISH signals could be detected. However, the first technique sometimes led to a loss of gene signals due to the reduction of the volume of the nuclei during the second cutting. The second technique could not always prevent the transferred sections from floating off the coated slides. This detachment seemed to depend on the thickness of the sections as it is well-known in immunohistochemistry and FISH and often cannot be cured even by using a coated slide. The third technique achieved the best results with no detachment of the transferred sections.

Conclusions: With the described techniques, it is possible to use routinely mounted and stained paraffin sections for additional examinations like FISH.

1560 Detection of B-RAF Activating Mutations in Malignant Melamona by High Resolution Amplicon Melting Analysis

C Willmore-Payne, JA Holden, LJ Layfield. University of Utah Health Sciences Center, Salt Lake City, UT.

Background: The B-RAF gene codes for a cytoplasmic serine/threonine kinase which is part of the mitogen activated protein kinase (MAPK) signaling cascade. Upon activation of RAS, B-RAF is recruited to the plasma membrane where if becomes phosphorylated to an active form. The activated B-RAF protein in turns phoshorylates several additional proteins in the MAPK pathway. The activation of this pathway eventually leads to transcriptional activation and cell growth. Recently, mutations have been identified in B-RAF that lead to constitutive activation. These mutations are particularly common in malignant melanoma and papillary thyroid carcinoma. The recent identification of RAF kinase inhibitors suggests that these novel drugs may be active in tumors harboring B-RAF activating mutations. In this study we used high resolution amplicon melting analysis to evaluate 82 cases of malignant melanoma for the presence or absence of B-RAF mutations.

Design: Eighty-two cases of malignant melanoma were retrieved from the surgical pathology files at the Unviersity of Utah Health Sciences Center. Genomic DNA was isolated from the paraffin blocks and subjected to polymerase chain reaction (PCR) with specific B-RAF exon 15 and exon 11 primers. After PCR, the samples were subjected to high resolution amplicon analysis performed with the HR-1 (Idaho Technology). An abnormal melting curve indicates an activating mutation. All cases were subsequently subjected to DNA sequencing.

Results: B-RAF activating mutations were found in 43 of 82 malignant melanomas (52%). In exon 15, 34 of the activating mutations were the common V600E (79%). Six cases showed a V600K (14%) and one case showed a V600R (2%). In exon 11, one case showed a G469V (2%) and one case showed a G469R (2%). Direct DNA sequencing confirmed that PCR products from an abnorml melting curve contained a mutation and PCR products from a normal melting curve contained a normal DNA sequence.

Conclusions: B-RAF activating mutations are common in malignant melanoma. They can be easily detected by high resolution amplicon melting analysis. Because the activating mutations are limited in number direct genotyping by high resolution analysis should be possible. The presence of B-RAF activating mutations in malignant melanoma could serve to identify a patient population that might benefit from therapy with RAF kinase inhibitors.

1561 CD10 Expression in Non-Hematopoietic Malignant Neoplasms: A Diagnostic Pitfall in the Working up of Metastatic Carcinoma of Unknown Origin

G Yue, YL Liu, M Tung, JF Silverman. Allegheny General Hospital, Pittsburgh, PA.

Background: Metastasis of unknown primary origin (MUO) constitute 5 to 10% of all non-cutaneous malignancies. Identifying the primary sites of MUO often requires extensive clinical and immunohistochemical studies. CD10 is a neutropeptidase which is expressed in acute lymphoblastic leukemia. Recently, CD10 positivity was also demonstrated in some epithelial malignancies (renal cell carcinoma, hepatocellular carcinoma) and endometrial stromal sarcoma. Moreover, CD10 is used to confirm these neoplasms as primary sites of MUO in histologic and cytologic specimens.

Design: A total of 82 cases of nonhematogenous carcinomas including stomach (11), colon (12), breast (11), lung (16), prostate (12), bladder (14) and pancreas(6) were retrieved from the hospital data base. Immunostaining for CD10 were performed on an automated immunostainer with appropriate positive and negative controls.

Results: CD10 expression was observed in a wide spectrum of non-hematopoietic malignant neoplasms including ductal adenocarcinoma of pancreas, transitional cell carcinoma of urinary bladder, prostatic adenocarcinoma, gastric adenocarcinoma, pulmonary adenocarcinoma, invasive ductal carcinoma of the breast and colon adenocarcinoma. No CD10 expression was detected in squamous cell carcinoma of lung.

Frequency of CD10 expression

Tumor	Prostate	Bladder	Stomach	Lung	Breast	Colon	Pancreas
CD10	100% (12/12)	86% (12/14)	82% (9/11)	56% (9/16)	18% (2/11)	50% (6/12)	33% (2/6)

Conclusions: We demonstrated that CD10 expression can be found in a wide variety of epithelial malignancies. When MUO is encountered in surgical pathology, caution should be taken in interpreting CD10 expression as a marker for RCC or hepatocellular carcinoma.

1562 Enzymatic Detection of Aneuploidy in Chromosomes 13, 18, 21, X and Y in Paraffin-Embedded Products of Conception

EL Zarovnaya, LS Tooke, K Ornvold, M Curtis, TK Mohandas, GJ Tsongalis. Dartmouth-Hitchcock Medical Center, Lebanon, NH; Third Wave Technologies, Madison, WI.

Background: Fetal aneuploidy of chromosomes 13, 18, 21, X or Y is most commonly associated with first trimester miscarriages. Current technologies used to detect common fetal aneuploidy include karyotyping, fluorescence in situ hybridization and polymerase chain reaction. Disadvantages of these technologies include labor intensiveness, length of time to culture cells, subjective grading and/or the need for fluorescent microscopy.

Design: In this study, we selected ten paraffin-embedded products of conception (POCs) that were submitted for routine histologic examination. All cases were reviewed by a pathologist. Aneuploidy was assessed using a prototype Aneuploidy Invader® Assay (Third Wave Technologies, Madison, WI) as a method to directly test extracted genomic DNA (PureGene kit, Gentra, Minneapolis, MN). This assay generates objective quantitative results by signal amplification using two different FRET cassettes containing spectrally distinct fluorophores for chromosomes 1, 13, 18, 21, X, or Y. All tissues were examined by routine cytogenetic analysis as the gold standard.

Results: Of the ten cases, two were detected as normal by the Aneuploidy Invader® Assay but were shown to be cytogenetically aneuploid for chromosomes 10 and 15 which are not detected by this assay. Trisomy 21 was detected in two cases by both methods as was trisomy 13 in one case. Two cases were correctly identified as 45XO (Turner's Syndrome).

Conclusions: While paraffin embedded tissues provide some challenges for this new method, the Aneuploidy Invader® Assay offers the advantage of rapid turn-around-time, increased throughput, and ease of performance. Our study suggests that this assay can be used on DNA extracted from paraffin-embedded tissues and may be complementary to routine cytogenetic studies.

1563 An Accurate Method for Determination of Tissue Thickness in Paraffin Blocks by Faxitron Analysis: Application to Tissue Microarray Construction

Y Zhao, X Kong, M Ksionsk, PD Walden, MC Bosland, J Melamed. NYU School of Medicine, New York, NY.

Background: The determination of tissue thickness in paraffin blocks in the histology laboratory has been largely based on visual estimates. More accurate methods are required for triage of paraffin embedded tissue for special studies and research applications. This is particularly crucial for tissue microarray (TMA) construction, where thin tissue from donor blocks can result in short TMA cores that are likely to disappear after few sections. Using an accurate method for thickness determination, one could include additional cores or avoid inadequate donor block material. We have developed an accurate method to determine thickness in donor paraffin blocks used for prostate cancer TMA construction as part of the NCI Cooperative Prostate Cancer Tissue Resource.

Design: Paraffin blocks of radical prostatectomy specimens (n = 247) assembled from 4 collaborating institutions were used for construction of 4 prostate cancer TMAs. All donor blocks were x-rayed after TMA construction using a digital Faxitron instrument, with vertical block alignment on the detector window. Digital radiograph images were manipulated to enhance contrast and to obtain linear measurements of the tissue at the TMA needle sites. The TMA blocks were cut into consecutive numbered 4 micron-thick sections through the entire block. The thickness of the individual cores determined radiographically was correlated with presence or loss of cores in the 150th TMA slide (from the final third of the TMA block).

Results: In the 150th slide derived from the 4 TMA blocks, 202 of 1388 cores (14.5%) were no longer present. The mean thickness of the paraffin embedded donor tissue corresponding to the absent cores was 1.54 mm as compared to 2.12 mm for the donor tissue corresponding to the preserved cores ($p< 0.01$). With increasing sections through a block, there was an increase in the number of lost cores with an inverse correlation between thickness of the donor block and loss of cores.

Conclusions: Accurate determination of tissue thickness in paraffin blocks can be obtained using Faxitron equipment which is available in many pathology laboratories. This type of determination is a valuable aid in construction of TMAs for large scale use. Prior knowledge of tissue thickness in TMA construction can prompt compensatory steps to enhance the yield of valuable samples and assure sufficient numbers of retained cores for statistical analysis in biomarker evaluations.

1564 Non-Invasive Prenatal RHD Genotyping by Real-Time PCR Using Plasma from RHD-Negative Pregnant Women

L Zhou, J Thorson, CE Nugent, RD Davenport, WJ Judd. University of Michigan, Ann Arbor, MI.

Background: Prenatal determination of fetal *RHD* genotype has become an important aid to the management of hemolytic disease of the newborn (HDN) due to maternal anti-D antibodies. Invasive procedures to obtain fetal genetic material for prenatal testing carry significant risks; therefore, non-invasive alternatives for the prenatal determination of fetal *RHD* genotype have been actively pursued. In this study we used a real time PCR-based assay to determine the fetal *RHD* genotype from cell free fetal DNA in maternal plasma.

Design: Peripheral blood samples were collected from 98 Rh-negative pregnant women. Cell-free DNA was extracted from the plasma and assayed for the presence of exons 4, 5, and 10 of the *RHD* gene by real-time PCR. The presence of fetal DNA in the samples was confirmed by the detection of the *SRY* gene on the Y chromosome in cases with a male fetus. If the PCR results for both the *RHD* and *SRY* genes were negative, the presence of fetal DNA was confirmed by demonstrating distinctions between cell free plasma DNA and maternal buffy coat DNA in their genotypes of 10 biallelic insertion/deletion polymorphisms. *RHD* genotyping results were compared with results from serological determination of the newborn's RhD phenotype.

Results: Seventy-two Rh-positive babies and 26 Rh-negative babies were identified by serological studies. *RHD* was detected in the maternal plasma of D-positive fetuses using exon 4, 5 and 10 primers in 69/72, 71/72, and 72/72 samples, respectively. None of the maternal plasma samples from the 26 Rh-negative fetuses were positive for *RHD* by the real time PCR assay. The presence of fetal DNA in the maternal plasma of D-negative fetuses was confirmed by the detection of *SRY* (10/10 boys). Distinctive genotypes for insertion deletion polymorphisms confirmed the presence of fetal DNA in 14 of 16 cases of female fetuses.

Conclusions: Using real-time PCR assays for the *RHD* gene in combination with assays for the *SRY* gene and a group of biallelic insertion/deletion polymorphisms, we obtained an accuracy of 94% in predicting fetal Rh D status in our study. Discrepancies between serology and PCR were attributable to the absence of amplifiable fetal DNA in a small number of maternal plasma samples. This assay provides a rapid and accurate assessment of fetal *RHD* genotype while avoiding the significant risks of invasive sampling procedures.

Ultrastructural

1565 Globular Hepatic Amyloid

N Agram, J Shia, D Klimstra, N Lau, R Erlandson, O Lin, D Filippa, T Godwin. Memorial Sloan-Kettering Cancer Center, New York; Washington Hospital Center, Washington, DC.

Background: Hepatic amyloid deposition in the form of globular inclusions is a rare occurrence. Its clinical and pathological significance is undefined, and its histologic appearance can cause diagnostic confusion.

Design: The clinical and pathological findings of a case of globular hepatic amyloid in a patient with B cell lymphoma and chronic hepatitis C are described, and relevant literature data is reviewed.

Results: The patient was a 64-year-old male, found to have abnormal liver function tests and positive HCV serology during a blood workup for his known B cell lymphoma. The lymphoma was diagnosed five years earlier and was in remission after chemoradiation. A liver biopsy to assess HCV disease revealed minimally active chronic hepatitis with mild periportal fibrosis. The liver also contained unusual intracytoplasmic globular inclusions within hepatocytes and stromal cells. These pale eosinophilic globules ranged from a few micrometers to 40 micrometers in diameter, and were homogeneous or laminated. Congo red stain and ultrastructural studies indicated that these globules were composed of amyloid. Linear form amyloid around vessels was also detected on Congo red stain and on EM. A subsequent fat pad fine needle aspiration demonstrated amyloid around vessels in the abdominal fat. Twenty-four reported globular hepatic amyloid cases have been described in association with a variety of medical conditions. Extra-hepatic organ involvement was not demonstrated in any of the reported cases except in one autopsy series. None of the reported cases were related to immunoglobulin light chain disease, nor did any patient present initially with clinical symptoms that would raise concern of amyloidosis.

Conclusions: Globular hepatic amyloid has a distinct morphologic pattern. Recognition of such a pattern is important in applying appropriate diagnostic modalities such as Congo red stain and electron microscopy. While the histogenesis of globular amyloid deposits remains undetermined, in some cases it may represent an early stage or mild form of systemic amyloidosis.

1566 Renal Tumors in Hereditary Leiomyomatosis Renal Cell Carcinoma Syndrome: Ultrastructural Characterization

A Ahmed, C Torres-Cabala, M Linehan, M Merino, M Tsokos. National Cancer Institute, Bethesda, MD; Center for Cancer Research, Bethesda, MD.

Background: Hereditary Leiomyomatosis Renal Cell Carcinoma (HLRCC) syndrome is a recently described familial syndrome characterized by germline mutations in the *fumarate hydratase* gene predisposing to multiple cutaneous and uterine leiomyomas and renal cell carcinoma . Renal cell carcinomas in patients with HLRCC have a distinct histology and aggressive clinical behavior. Their ultrastructural features have not been previously described.

Design: Tissue from three renal tumors from three patients with confirmed HLRCC syndrome was studied. Representative areas from all three tumors were fixed in buffered glutaraldehyde and processed for ultrastructural analysis.

Results: All three patients were males 40 (two patients) and 64 years of age and had undergone nephrectomy procedures. Two of them were members of the same family. Metastatic disease in the surrounding muscles and omentum was present in two cases. The tumors had a spectrum of morphologic changes including papillary type II morphology with cystic and solid areas. The characteristic nuclear appearance was present in all three cases. All tumors exhibited common ultrastructural features. Specifically, they were composed of clusters of cuboidal cells forming tubular structures and surrounded by multilayered basal lamina. The tumor cells exhibited short apical villi and basal infoldings. The intercellular spaces were widened. The cytoplasm contained numerous mitochondria and abundant often dilated endoplasmic reticulum. Lipid droplets were variable but usually seen in low amounts. Glycogen and lysosomes were present as well. The nuclei were irregular and often exhibited prominent nucleoli. One tumor exhibited in addition some intracytoplasmic vesicles and sparse clusters of intermediate filaments indicative of tonofilaments. Inter-epithelial junctions were common.

Conclusions: Renal tumors in HLRCC patients have unique ultrastructural features suggestive of origin from distal segments of the nephron. They also have a high mitochondrial content, possibly due to their genetic abnormality in an enzyme involved in the Krebs cycle.

1567 Adult Benign Cystic Renal Lesions-Electron Microscopic Studies with Histogenetic Correlations

T Antic, R Fresco, MM Picken. Loyola University Medical Center, Maywood, IL.

Background: Adult cystic nephroma (ACN) is a rare tumor composed of cysts separated by thin septa containing loose stroma with fibroblasts and, focally, cells resembling smooth muscle. The epithelial lining in ACN is hobnail or attenuated and an origin in the distal nephron has been postulated. Mixed epithelial and stromal tumor of the kidney (MESTK) is a recently recognized rare tumor composed of intimately admixed tubules and spindle cell stroma that resembles ovarian. The tumor is usually benign and no blastema, mitoses or atypia are seen. The tumor origin is debated and recently an origin in the distal nephron has been postulated.

Design: We performed detailed morphologic studies, including routine histology, immunohistochemistry and electron microscopy (EM) in four benign adult cystic lesions. Three tumors were classified as MESTK and one as ACN. All tumors were from females.